nanomat

Universidad Zaragoza · Ciencias Zaragoza · icma

Masters Degree in
Nanostructured Materials for
Nanotechnology Applications

University of Zaragoza

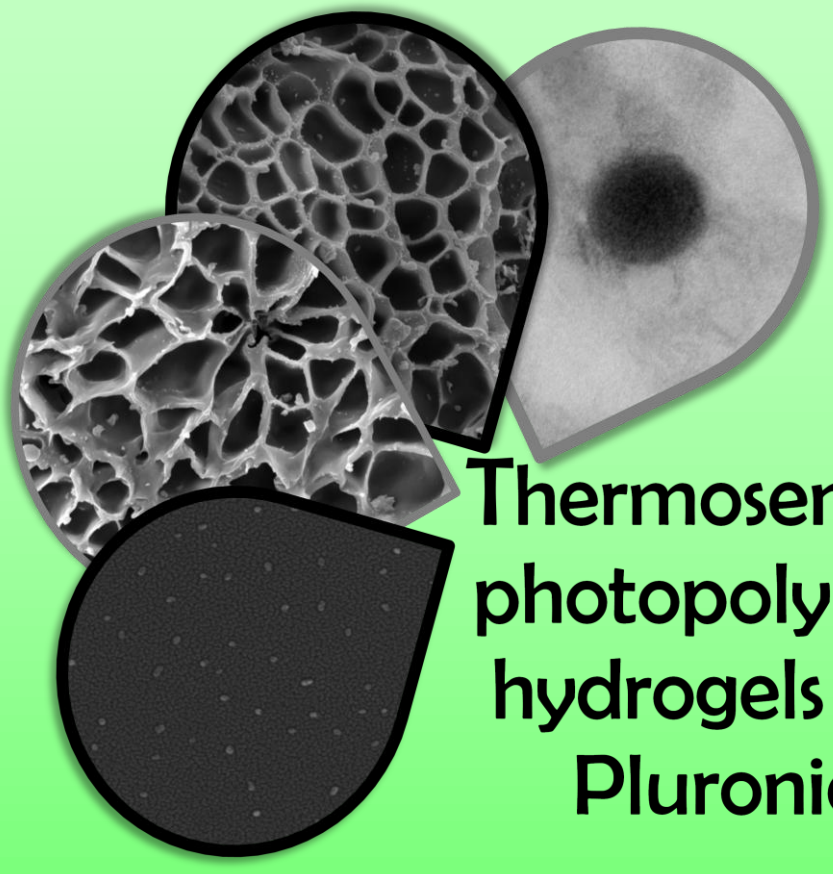

# Thermosensitive and photopolymerizable hydrogels based on Pluronic® F127

## Final Master Project

Student: I.Lucía Herrer Jiménez

Directors: Dr. M.Blanca Ros and Dr. Teresa Sierra.

Research group: Liquid Crystals and Polymers. Organic chemistry dept.

The supervisors of this project: Dr. María Blanca Ros Latienda (Full professor of the University of Zaragoza) and Dr. Teresa Sierra Travieso (Scientific Researcher of the CSIC), of the Institute of Materials Science of Aragon (University of Zaragoza-CSIC),

**CERTIFY**

That the present work called **"Thermosensitive and photopolymerizable hydrogels based on Pluronic® F127"** has been carried out by **I. Lucía Herrer Jiménez** under our supervision. This document reflects the work done as the Final Master Project to obtain the Master Degree in Nanostructured Materials for Nanotechnology Applications of the University of Zaragoza.

Zaragoza, 9th September 2013

Dr. María Blanca Ros Latienda

Dr. Teresa Sierra Travieso

## ABSTRACT

Here it is reported the design, synthesis and characterization of new Pluronic® F127 derivatives, with the ability to form thermosensitive and photopolymerizable hydrogels. These active hydrogels undergo a sol-to-gel transition by increasing the temperature in a physiologically important temperature range thus resulting attractive for biomedical applications and drug delivery systems. Pluronic® F127 has been functionalized with photoreactive groups and the obtained derivatives and their precursors have been fully characterized by conventional techniques. Then the aimed compounds have been processed as macroscopically molded hydrogels and as nanostructured hydrogels (nanogels). A highly crosslinked internal structure has been reached by the photopolymerization technique for the thermosensitive macroscopic hydrogels designed to act as cell scaffolds for cartilage repair. Swelling and degradation studies as well as their morphological characterization by SEM have been carried out. Concerning the nanostructured hydrogels (nanogels), after determining its critical micellar concentration and applying a photopolymerization process to fix the nanostructure, they have been characterized by TEM, SEM and DLS. Cell viability assays have been carried out for both types of system, the macroscopic hydrogel and the nanogel.

## Acronyms

| | |
|---|---|
| **CGC** | Critical gelling concentration |
| **CMC** | Critical micelle concentration |
| **CMT** | Critical micelle temperature |
| **DLS** | Dynamic light scattering |
| **DCS** | Differential scanning calorimetry |
| **DCM** | Dichloromethane |
| **DMEM** | Dulbecco's Modified Eagle's Medium |
| **GPC** | Gel permeation chromatography |
| **IHs** | Injectable hydrogels |
| **IR** | Infrared |
| **LCST** | Lower critical solution temperature |
| **MALDI** | Matrix-Assisted Laser Desorption/Ionization |
| **MS** | Mass spectrometry |
| **MSC** | Mesenquimal stem cells |
| **NMR-$^{1}$H** | Proton nuclear magnetic resonance |
| **NMR-$^{13}$C** | Carbon nuclear magnetic resonance |
| **PBS** | Phosphate buffered saline |
| **SEM** | Scanning electron microscopy |
| **TEM** | Transmission electron microscopy |
| **TIM** | Test-tube inverting method |
| **UV** | Ultraviolet |

## INDEX

# 1. INTRODUCTION

- Hydrogels

Hydrogels are three-dimmensional polymeric networks which can swell in water and hold a significant amount of water, while maintaining their shape and structure. According to the type of driving force leading to crosslinking network, hydrogels are divided by physical or chemical hydrogels, which correspond to non-covalent or covalent interactions, respectively[1]. One of the techniques to form chemically crosslinked hydrogels is by photopolymerization. Photopolymerization is a process whereby light interacts with light-sensitive compounds called photoinitiators, to create free radicals that can initiate the polymerization of monomers to form crosslinked hydrogels in a fast manner under ambient or physiological conditions[2].

Nowadays, sensitive hydrogels with specific response to various environmental stimuli are being a topic of extensive research. Among these sensitive hydrogels are the thermoresponsive hydrogels.

A thermoresponsive hydrogel utilize a temperature change as the trigger that determines its gelling behavior without any additional external factor[3]. For these hydrogels, the phenomenon of transition from a solution to a gel is commonly referred to as sol-gel transition. Within thermoresponsive hydrogels, there are some of them that exhibit a separation from solution (sol state) and the gel state above a certain temperature. This threshold is defined as the lower critical solution temperature (LCST), which means that the hydrogel is formed upon heating the solution. Concretely, some thermoresponsive hydrogels undergo a sol-to-gel transition in a physiologically important temperature range of 10-40 ºC[4], this is the reason why these hydrogels are very interesting for biomedical uses, providing the advantage of an easy administration as they can be injected in the sol state achieving *in situ* the gel state under physiological conditions. This behavior led to what is now known as injectable hydrogels (IHs).

An important class of thermoresponsive hydrogels are a type of block copolymers formed by blocks of poly(ethylene glycol) (PEG) and poly(propylene glycol) (PPG), known as Pluronics (BASF trade name) or Poloxamers (ICI trade name), namely triblock structures of poly(ethylene glycol-b-propylene glycol-b-ethylene glycol). In a

water environment, due to their amphiphilic character, most Pluronics form ordered aggregates, most commonly micelles5. These materials are utilized for various biomedical applications due to low toxicity and their amphipilic properties[6]. These block copolymers in aqueous solution undergo a thermosensitive sol-to-gel transition with LSCT[7].

The unique properties of the thermogelling materials have recently been investigated as a platform technology enabling: minimally invasive drug delivery system, three-dimensional cell culture and injectable tissue engineering using mesenchymal stem cells, post-surgical treatments for adhesion prevention, long-term magnetic resonance imaging contrasting, transcatheter arterial embolization and 3D live cell imaging for cellular processes[8].

The present research work deals with new Pluronic® derivatives, and focuses on two of these applications envisaged for thermosensitive hydrogels: Hydrogels for tissue repair and nanostructured hydrogels for drug delivery.

- LCST hydrogels for tissue repair

A major goal of hydrogel-based technology is the development of injectable hydrogels (IHs)[9], where an aqueous mixture of gel precursors and bioactive agents is administered using a syringue and gelates inside the body due to the temperature change. Due to its high moldability, they offer the possibility of *in vivo* delivery in a minimally invasive way and also on the capacity of easy and effective encapsulation of cells and/or drugs[9].

Within the field of tissue engineering, IHs are being broadly investigated to act as a scaffold material for cartilage regeneration[10].

Cartilage lesions are potentially a major cause of joint disease and disability affecting millions of people all over the world as they can lead to osteoarthritis. Injuries and degenerative changes in the articular cartilage are a significant cause of morbidity and diminished quality of life. Concretely, it is expected that by the year 2030, 67 million (25%) adults will have diagnosed arthritis and the 37% (25 million adults) of those with arthritis will report arthritis-attributable activity limitations[11].

The current treatment options for cartilage injuries include microfracture of the subchondral bone, joint lavage, tissue debridement, transplantation of autologus or allogeneic osteochondral grafts. The success rate of these treatment procedures is not consistent and they vary greatly. Some of these techniques show promise of cartilage regeneration while others lead to the formation of fibrous tissue, apoptosis and further degeneration of cartilage[12].

Once a cartilage begins to degenerate, the repair process is very slow and in the majority of cases the tissue is not entirely replaced. This is due to the fact that cartilage lacks the capability of repairing itself, because of its low vascularity, and low chondrocyte activity. This is the reason why the use of tissue engineering methods to repair cartilage has become a very attractive option. The ultimate goal is to implant a scaffold that can persist in a robust state for sufficient time to allow for the formation of new tissue, but which will degrade and become replaced by this tissue.

- Nanostructured hydrogels, i.e. nanogels

From a different point of view, another important application of hydrogels involves their use as nanocarriers for drug delivery. The term ‘‘nanocarrier’’ is used to describe hybrid multifunctional systems with sizes typically ranging between 1–200 nm, which may deliver the bioactive agent at the targeted site with improved therapeutic activity over the free form of bioactive agent[13]. The term “nanogels” usually defines aqueous dispersions of hydrogel particles formed by physically or chemically cross-linked polymer networks of nanoscale size[14].

Nanogels are very promising as drug-delivery carriers because of their high loading capacity, high stability, and responsiveness to environmental factors, such as ionic strength, pH, and temperature that are unprecedented for common pharmaceutical nanocarriers. The main property of the amphiphilic polymers used to prepare nanogels, is that they can form a micellar structure with a hydrophobic compact inner core and a hydrophilic swollen outer shell in aqueous environments[15].

## 2. OBJECTIVE

The final aim of this work is the design, synthesis and characterization of new amphiphilic block-copolymers, which have the ability to form thermosensitive and

photopolymerizable hydrogels. These materials will be processed as macroscopic hydrogels to be used as scaffold for cell culture to tissue engineering applications and as nanostructured hydrogels (i.e. nanogels) as drug delivery systems.

The objective and work plan of this Master project lies within the frame of the aim and subjects of the Master Degree in Nanostructured Materials for Nanotechnology Applications *(http://titulaciones.unizar.es/asignaturas/66110/contexto12.html)*. Indeed, the work gathers the synthesis of new molecules that enable the preparation of nanostructured materials. Furthermore, the characterization of the newly prepared materials is based on techniques learned as suitable for nanosized systems.

## 3. PLANNING

The plan followed in the realization of this work is summarized in the following steps:

**1º) Design, synthesis and characterization of the target molecules**:

Starting with the commercial polymer Pluronic® F127, "P", the plan was to synthesize two different carbamate-derivatives that incorporate photoreactive groups: a linear block copolymer derivative, named "P/A-2" and a hybrid dendritic-linear-dendritic block copolymer derivative, named "P/A-4".

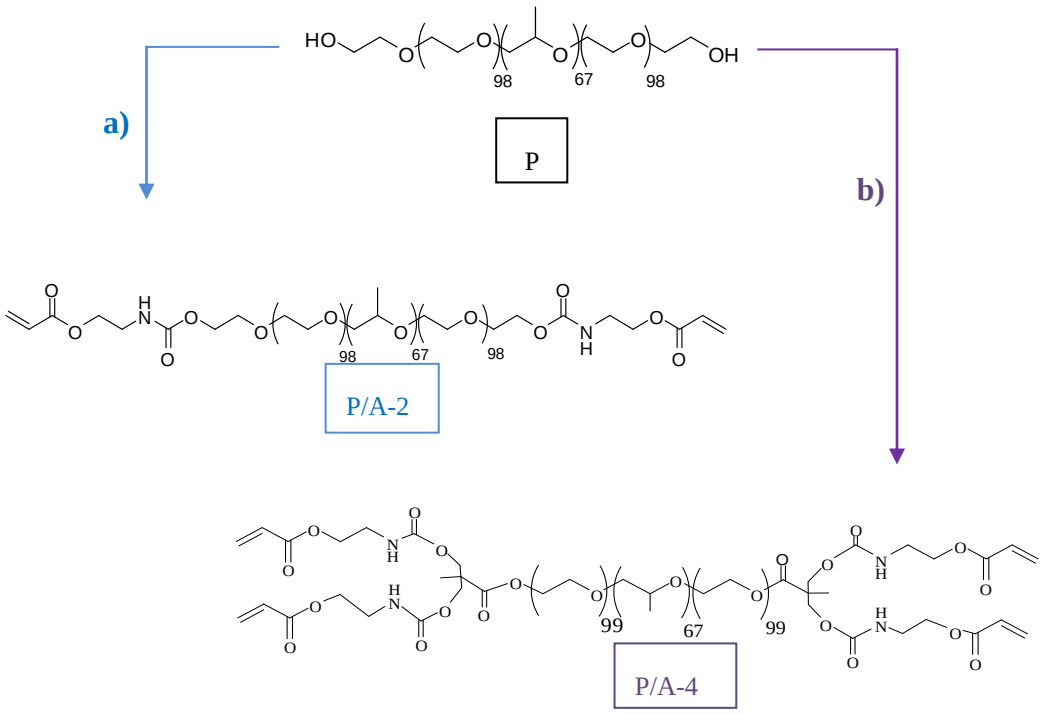


*Scheme 1. Chemical structure and nomenclature of the aimed compounds.*

Both compounds, as well as the intermediates would be characterized by using $^{1}$H-RMN, $^{13}$C-RMN, FT-IR, MALDI and GPC.

The nomenclature used, e.g. P/A-2, has two parts. The first one, *P*, refers to the structural core of the product, which is based on the structure of the original material, commercial Pluronic® F127. The second part, *A-2*, refers to the new lateral groups introduced in the structure of pluronic by several synthesis steps, and also refers to the number of these groups. In this particular case, the letter *A* means acrylate, and the number *2,* means that there are two acrylate groups at the end of the molecule, one on each side.

**2º) Sol-gel studies:**

The second step of the work was to prepare macroscopic hydrogels in order to analyze the gelation properties of the new compounds.

**3º) Photopolymerization:**

Hereinafter, it was planned to fix the gel structure of reactive materials through photopolymerization techniques, either as a macroscopic hydrogels and as a nanogel (nanostructured hydrogel).

**4º) Hydrogel characterization:**

The internal morphology of the macroscopic hydrogel will be studied by SEM. The nanogel size and morphology will be studied by TEM, SEM and DLS. Furthermore, degradation tests of the macroscopic hydrogels will be studied.

**5º) Cell viability studies:**

Finally, in the aim of biological applications of these materials, cell viability studies are also planned, either as a macroscopic hydrogels, and also as a nanogels.

# 4. RESULTS AND DISCUSSSION

## 4.1.- SYNTHESIS AND CHARACTERIZATION

### 4.1.1) Synthesis of the linear Pluronic derivative, *P/A-2.*

In order to synthesize product P/A-2, the synthetic route followed is shown in Scheme 2:

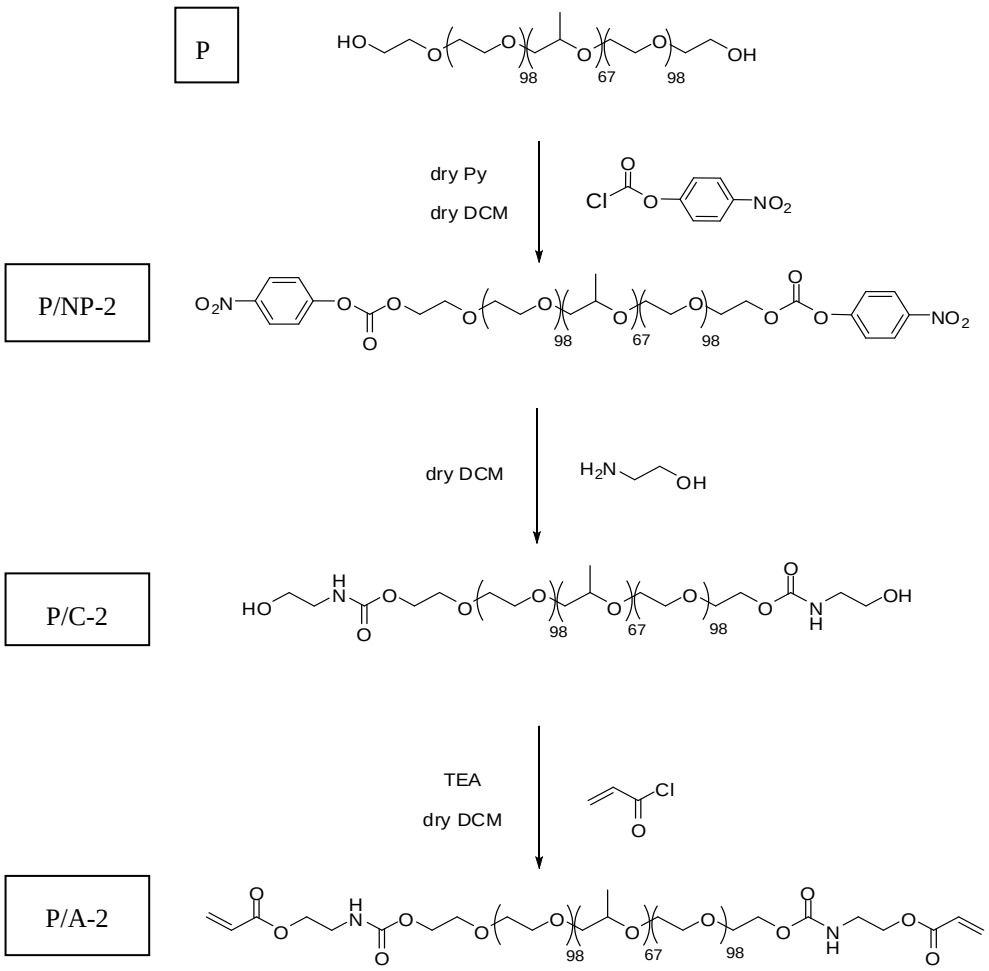


*Scheme 2. Synthetic route of compound P/A-2*

With the purpose to check and prove the correct functionalization in each synthesis step, $^{1}$H-NMR has been used in order to follow the appearance or disappearance of the main characteristic signals corresponding to each molecule, as shown in Figure 1.

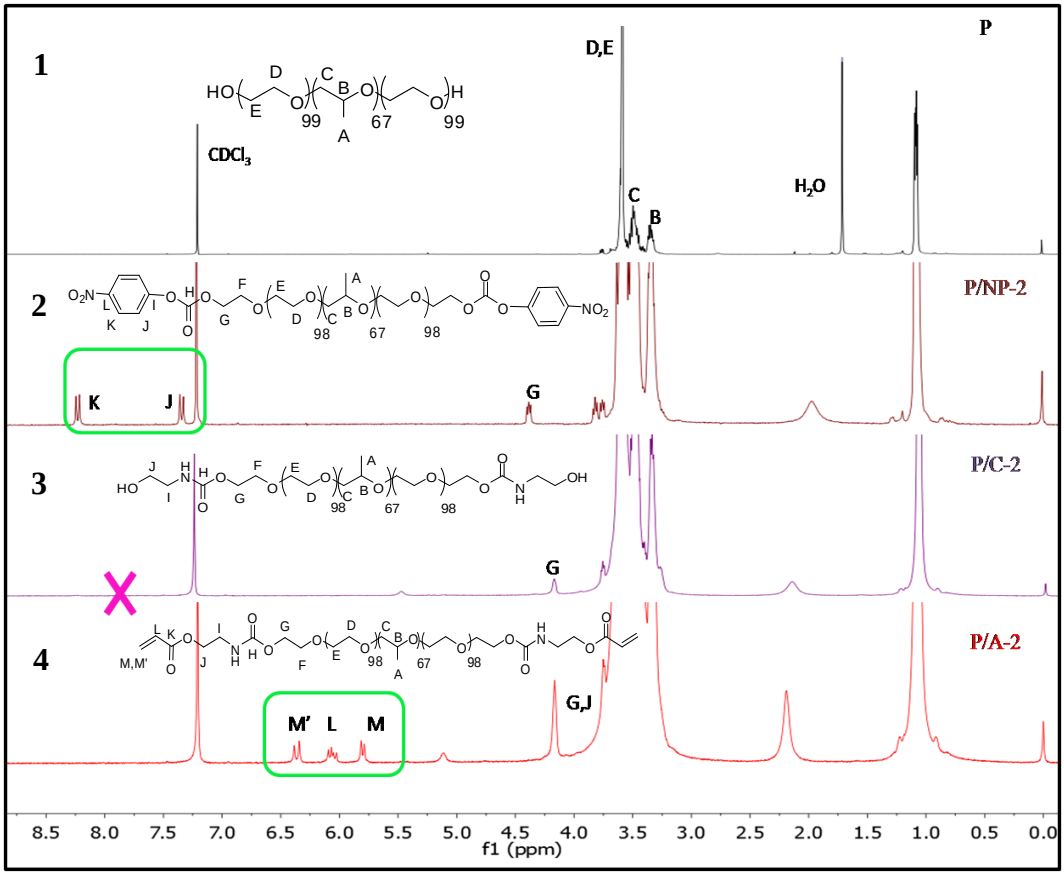


*Figure 1. [1]H-NMR spectra of commercial Pluronic F127 (P), P/NP-2, P/C-2, and P/A-2, respectivelly.*

In the [1]H-NMR spectrum of the P/NP-2 compound (spectrum 2 in Figure 1), three new characteristic signals appear with respect to P. First, the multiplet at 4.41 ppm which corresponds to PEG chain protons directly linked to the newly formed carbonate group (G protons). The other two characteristic signals are at 7.39 ppm (J protons) and 8.27 ppm (K protons) corresponding to the aromatic protons. These aromatic signals help to follow the next reaction due to its complete disappearance in the spectrum of the compound P/C-2 (spectrum 3 in Figure 1).

Finally, in the last spectrum (spectrum 4 in Figure 1), corresponding to the P/A-2 molecule, two significant changes are appreciated: three doublets of doublets between 5.84 and 6.44 ppm, which are the signals of the introduced acrylate groups (M, L and M'), and the multiplet at 4.22 ppm corresponding now to G protons and J protons.

The molecule P/C-2 is difficult to characterize only by $^{1}$H-NMR because meaningful protons are mobile protons, then, another useful tool to check the changes within the molecule was infrared spectroscopy (IR), as shown in Figure 2.

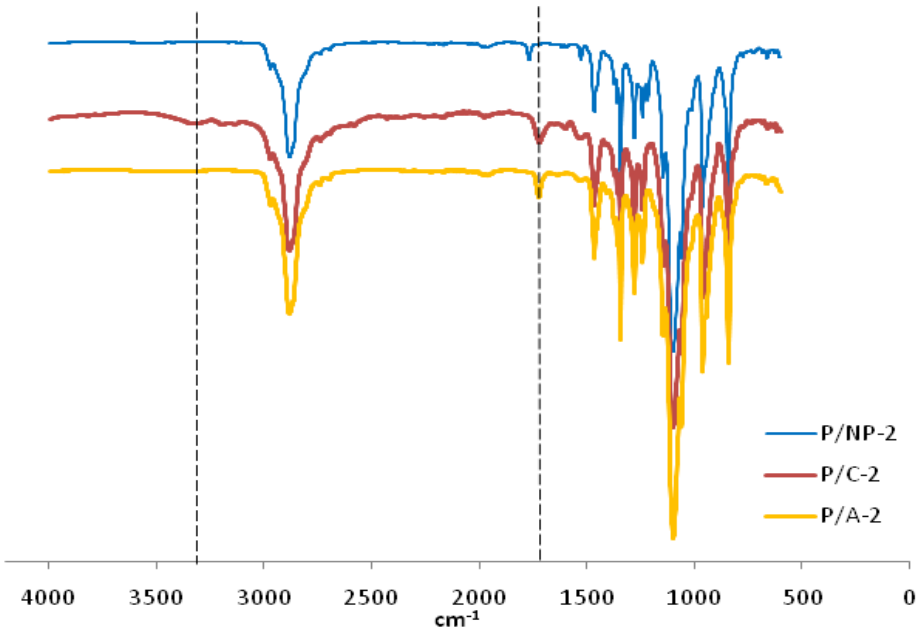


*Figure 2. FTIR-ATR spectra of P, P/C-2 and P/A-2 respectively.*

In the IR spectrum of the P/C-2 compound (red spectrum in Figure 2), it can be appreciate a band between 3500-3250 $cm^{-1}$ corresponding to the O-H st, which help to confirm the structure of the molecule. Also, another important signal which can be compared between the molecules, is the band appearing at 1765 $cm^{-1}$ for the P/NP-2 compound (blue spectrum in figure 2), corresponding to the C=O st from carbonate, and at 1722 $cm^{-1}$ and at 1728 $cm^{-1}$ for the compound P/C-2 and P/A-4, respectively, corresponding to the C=O st from carbamate.

Also, mass spectrometry (MS) has been used to study the compounds P/C-2 and P/A-2 to prove the mass changes with respect to the original material, P.

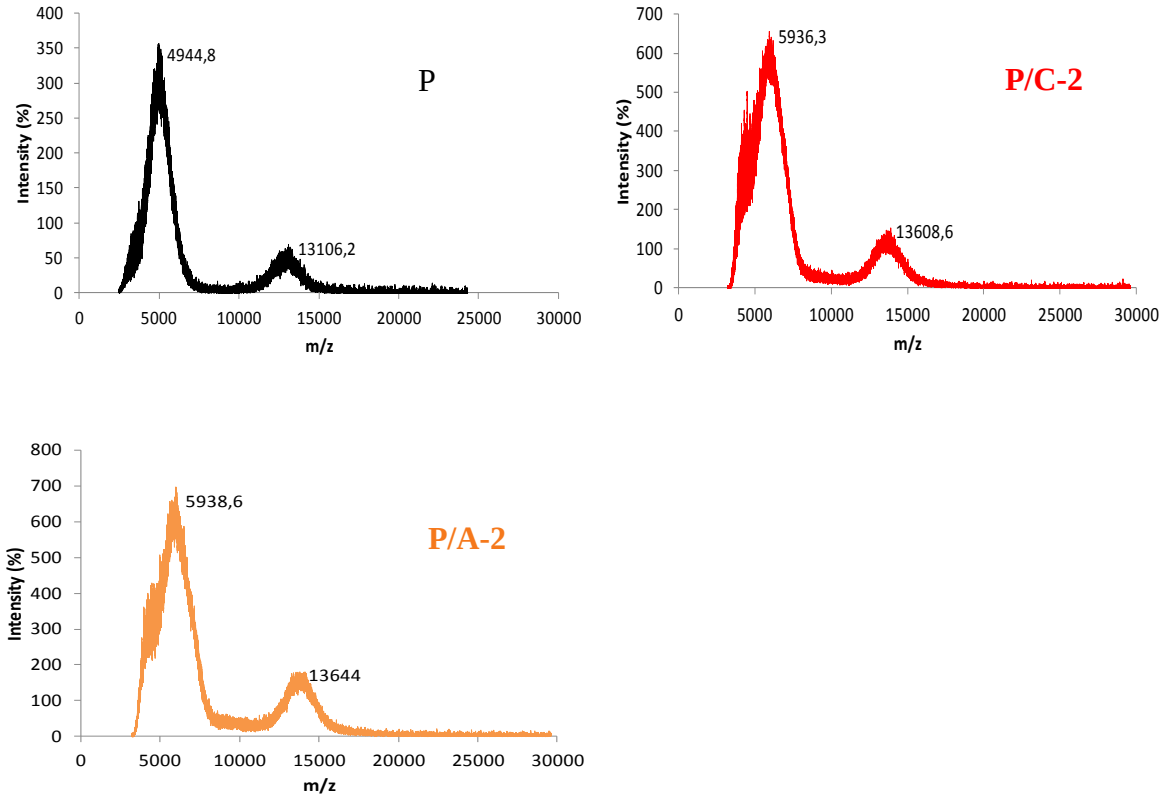


*Figure 3. MS of P and its derivatives.*

In Figure 3, a displacement of the mass distribution towards higher mass/charge relationship is observed, which is due to the functionalization carried out at the initial polymer, P.

Finally, both compounds were characterized by Gel Permeation Chromatography (GPC), using polystyrene standards for calibration. (see Figure 4)

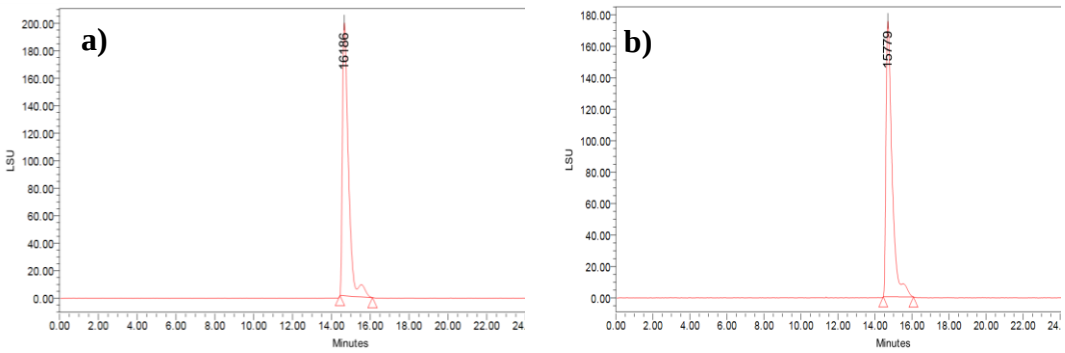


*Figure 4. Obtained chromatograms by GPC for a) P/C-2 compound and b) P/A-2 compound.*

The obtained data are presented in Table 1.

*Table 1. Obtained data from GPC experiments performed with Styrage® columns HR1.*

| | **$M_n$ [a]** | **$M_w$** | **PDI [b]** | **$M_W$[c] calculated (g/mol)** |
|---|---|---|---|---|
| **Pluronic F127** | 16748<br>6438 | 17193<br>7105 | 1.03<br>1.1 | 12600 |
| **P/C-2** | 13898 | 14621 | 1.05 | 12774 |
| **P/A-2** | 13445 | 14159 | 1.05 | 12882 |

[a]$M_n$ : number average molecular weight (g/mol) obtained by GPC.
[b]PDI: polidispersity index ($M_w/M_n$) obtained by GPC.
[c]MW calculated: molecular weight in g/mol, calculated as the sum of the molecular weight of individual blocks.

Commercial Pluronic F127 shows a chromatogram with two different molecular weight distributions (see Appendix 1). The new materials show also two distributions in their chromatograms, but they are not so well separated, this behavior could be associated to the new functionalization present in the molecules.

The new materials show two distributions in their chromatograms corresponding to two molecular weight distributions as shown by the commercial Pluronic F127 (see Appendix 1). Also, as indicated in Table 1, comparing the obtained values from GPC referring the calculated ones, $M_W$ (last column of Table 1), we find differences. These differences can be attributed, in one side to the fact that calibration is made with a different polymer, polystyrene, which has a different hydrodynamic volume. On the other side, different variables to take into account are how the polymer behaves within the column, and the polymer's molecular weight.

The use of this technique also allows us to verify the presence of two molecular weight distributions in both materials, as previously noted by MS.

### 4.1.2) Synthesis of the hybrid dendritic-linear-dendritic block copolymer (HDLDBC), P/A-4.

The synthetic route followed to prepare the compound P/A-4 is shown in Scheme 3:

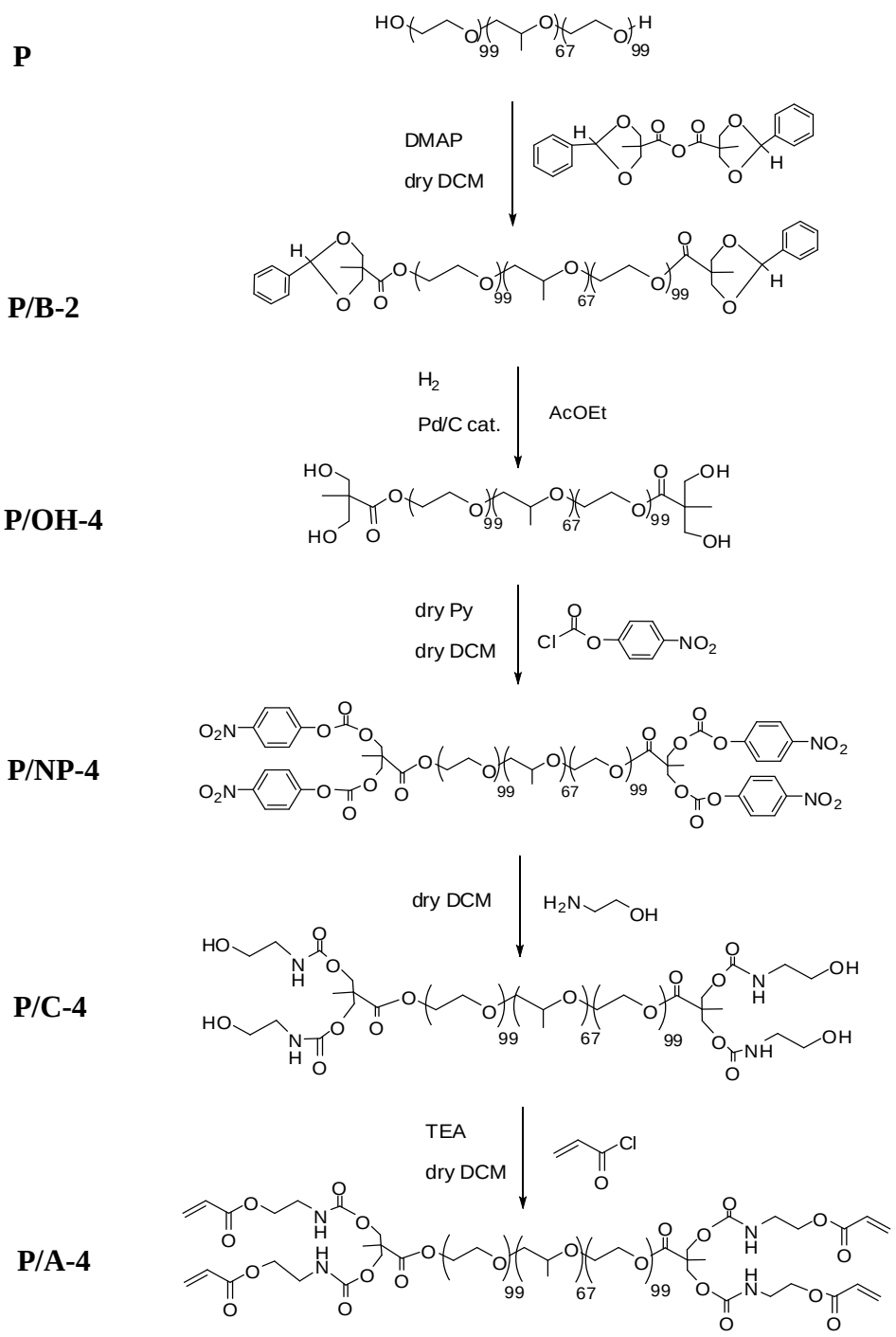


*Scheme 3. Synthetic route of compound P/A-4.*

The products P/B-2, P/OH-4, P/NP-4, and P/C-4 have been correctly obtained and isolated, but, the optimal experimental conditions to obtain the final product, P/A-4 have not been stated so far.

After using different strategies, the full functionalization of the ending hydroxyl groups of P/C-4, was not reached. In all attemps, a certain degree of functionalization, but not constant, was observed. The best results, even though functionalization was not complete, were achieved using tetrahydrofuran as solvent instead of dichloromethane. The optimization of this reaction is still in progress.

## 4.2.-SOL-GEL STUDIES

The sol-gel properties have been studied for the following materials:

-Commercial Pluronic F127.

-Linear Pluronic derivative, P/A-2 and its precursor, P/C-2.

For each material, aqueous solutions with five different concentrations (w/v) have been tested, i.e. 16 %, 18 %, 20 %, 23 %, and 25 %. (Experimental section 5.3)

The study of these properties is based in the application of two different methods to determine the Low Critical Solution Temperature, (LCST):

- Test-tube inverting method (TIM):

This simple method was employed to roughly determine the sol-gel transition temperature. When the test-tube, or vial, containing the solution, is inverted, it is defined as a sol phase if the solution deforms by flow, or a gel phase if there is no flow. Accordingly, the LCST was defined as the temperature when the material doesn't flow during at least 10 seconds when the vial is upside down.

Also, in this experiment the materials were heated above the LCST, to find the temperature at which the material became again a sol, after reaching the gel state, what has been called *gel-sol transition.*

- Differential Scanning Calorimetry (DSC):

DSC is a thermoanalytic technique that allows determining sol-gel transition temperatures, and which has been already used for the study of Pluronic F127 [16, 17].

In our case, for each studied material, the same samples prepared for the TIM, have been studied by DSC technique.

The obtained thermograms allow the recognition of two different signals, corresponding to the micellization and gelation processes (Figure 5).

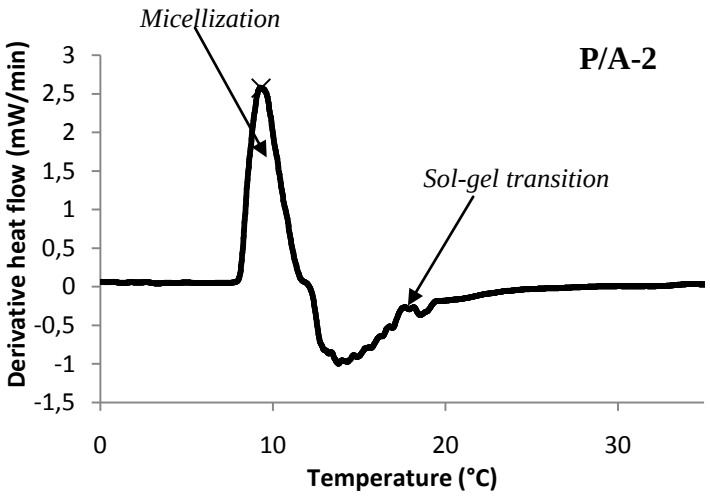


*Figure 5. Example of obtained thermograms from P/A-2 material, illustrating the micellization and gelation processes.*

The main peak corresponds to the micellization process. It allows to know the critical micellization temperature (CMT), at which the aggregation of the polymeric chains, for a particular concentration takes place.

As it may be appreciated in Figure 5, the gelation peak appears as a small peak at higher temperature, this peak is only well defined when the polymer concentration is high, usually 25 %(w/v)[18], for smaller concentrations this peak is not so well defined.

In the cases where the gelation peak was not clearly appreciated in the thermogram, but the material showed sol-gel properties, we stated as the value for LCST as the temperature at which it is considered that the gel is entirely formed, corresponding this temperature with the stabilization of the baseline in the thermogram ( Figure 6).

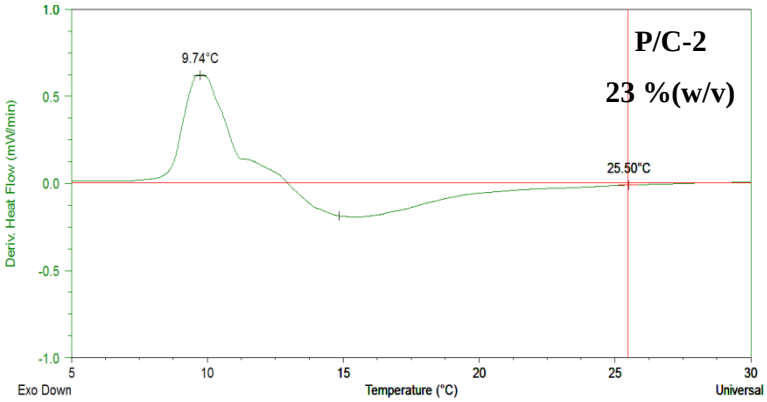


*Figure 6. DSC thermogram obtained for the material P/C-2 at 23 % (w/v). Example to illustrate how the LSCT is determined for materials where the gelation peak is not detected.*

The obtained DSC thermograms for all the studied materials are presented in Appendix 2.

### 4.2.1 .- Sol-Gel properties of commercial Pluronic F127

Figure 7 shows the phase diagram of this material, which shows how Pluronic F127 behaves depending on concentration and temperature.

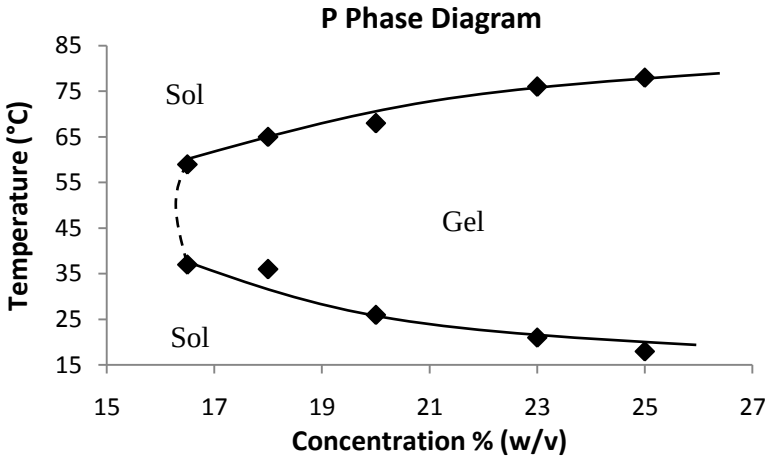


*Figure 7. Phase diagram for Pluronic F127, obtained from TIM.*

Table 2 summarizes the sol-gel properties obtained from the application of the two above-commented methods, the test-tube inversion method (TIM) and the differential scanning calorimetry (DSC).

*Table 2. Summary of the obtained data for Pluronic F127 with TIM and DSC methods.*

| % [P] | Micellization Temp. (°C) (Obtained by DSC) | LCST (gelation process)(°C) | | | Gel-sol transition (°C) |
|---|---|---|---|---|---|
| | | TIM | DCS (baseline)* | DCS (gel peak) | TIM |
| 16,5 | 14 | 37 | 32 | - | 59 |
| 18 | 13 | 36 | 30 | - | 65 |
| 20 | 11 | 26 | 25 | - | 68 |
| 23 | 10 | 21 | 26 | 18 | 76 |
| 25 | 9 | 18 | 30 | 17 | 78 |

*Data obtained as illustrated in Figure 6.

### 4.2.2 .- Sol-Gel properties of P/C-2

Results concerning the gelling properties for P/C-2 are shown in Figure 8 and Table 3.

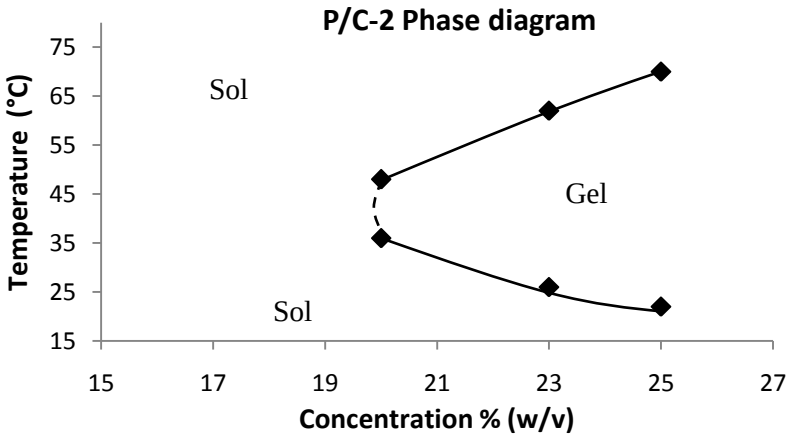


*Figure 8. Phase diagram for P/C-2 , obtained from TIM.*

*Table 3. Summary of the obtained data for P/C-2 with TIM and DSC methods.*

| % [P/C-2] | Micellization T. (°C) | LCST (gelation process)(°C) | | Gel-sol transition (°C) |
|---|---|---|---|---|
| | | TIM | DCS (baseline)* | TIM |
| 16 | 13 | no gel | no gel | - |
| 18 | 13 | no gel | no gel | - |
| 20 | 11 | 36 | 29 | 48 |
| 23 | 10 | 26 | 25 | 62 |
| 25 | 9 | 22 | 25 | 70 |

*Data obtained as illustrated in Figure 6.

Compound P/C-2, which has hydroxyl groups as terminal groups in both parts of the molecule, shows a different behaviour in terms of gelation properties compared to Pluronic F127. Indeed, it is necessary, due to the chemical modification within the molecule, to increment the concentration of the compound up to 20% (w/v) to obtain a hydrogel.

### 4.2.3.- Sol-Gel properties of P/A-2

Finally, results concerning the gelling properties for P/A-2, are shown in Figure 9 and Table 4.

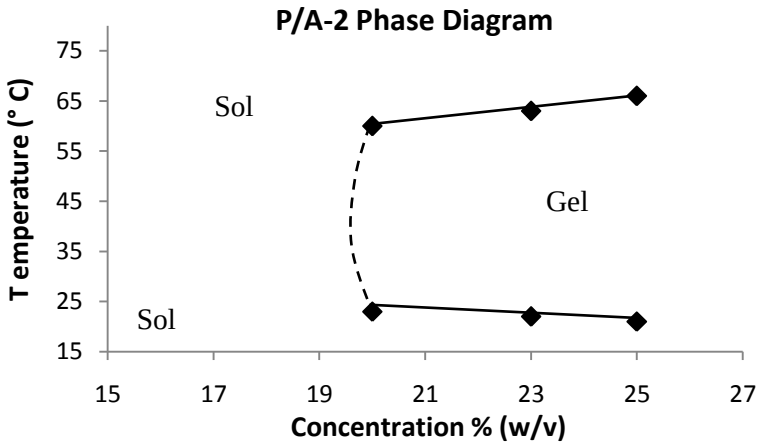


*Figure 9. Phase diagram for P/A-2, obtained from TIM .*

Compounds P/C-2 and P/A-2 behave similarly with respect to the critical gelling concentration (CGC), 20 % (w/v), which is not affected by the fact of changing the size of the side groups of the molecule. However, for P/A-2 the temperature range for the gel state is bigger than for compound P/C-2. This leads us to conclude that the presence of acrylate groups allows the stabilization of the gel.

*Table 4. Summary of the obtained properties for P/A-2 with TIM and DSC methods.*

| | | LCST (gelation process)(°C) | | | Gel-sol transition |
|---|---|---|---|---|---|
| % [P/A-2] | Micellization T. (°C) | TIM | DCS (baseline)* | DCS (gel Peak) | TIM |
| 10 | 17 | no gel | no gel | no gel | - |
| 16 | 14 | no gel | no gel | no gel | - |
| 18 | 15 | no gel | no gel | no gel | - |
| 20 | 9 | 23 | 23 | 14 | 60 |
| 23 | 10 | 22 | 24 | 20 | 63 |
| 25 | 9 | 21 | 24 | 18 | 66 |

*Data obtained as illustrated in Figure 6.

Finally, it is necessary to remark, that the obtained results from TIM and DSC, for the three studied compounds, are not completely comparable between them. This can be attributed to the fact that the determination of the LCST, is strongly dependent on the amount of sample used for the experiment, as well as of the sample's container geometry[19] , and here, the container used in each of the techniques, is different (see Experimental section 5.3).

## 4.3 PHOTOPOLYMERIZED HYDROGELS

This section is organized in two parts, which are related with the two aimed applications of the thermosensitive hydrogels prepared

- The first part shows the results concerning the compound P/A-2, and corresponds to the formation of the chemically crosslinked macroscopic hydrogels, to be used as scaffolds for cell culture.
- The second part shows the results concerning the preparation of nanostructured hydrogels (nanogels) to be used for molecular encapsulation applications.

### 4.3.1.MACROSCOPIC HYDROGEL

#### 4.3.1.1.-Photopolymerized hydrogel

To produce the crosslinked photopolymerized hydrogel, compound P/A-2, was disolved in a PBS solution containing a certain amount of Irgacure 2959 photoinitiator. The

polymerized macroscopic structures (Figure 10) were obtained as detailed in Experimental section 5.4.

In this study, concentrations to carry out the photopolymerized hydrogels with the P/A-2 material of 20% and 23% (w/v) were chosen, because as seen previously, these were the concentrations where the material shows gel characteristics.

*Figure 10. Obtained photopolymerized hydrogel after demould it. Material: P/A-2, 23% (w/v).*

#### 4.3.1.2.-Morphological characterization

To characterize the internal morphology of the photopolymerized hydrogel derived from P/A-2, scanning electron microscopy (SEM) has been used.

To prepare the samples, the obtained hydrogel with the fixed structure (See Experimental section 5.4) was equilibrated for 3 days in 2 ml of PBS 10 mM, pH= 7.4. Then, in order to fracture the gel and keep the internal structure intact for a properly characterization, it was necessary to freeze the gel by using liquid nitrogen, once broken, the sample was lyophilized overnight.

Before carrying out the SEM experiments, the sample was fixed on a carbon tape, and coated it with gold.

Figures 11 and 12 gather SEM images obtained for photopolymerized hydrogel prepared from two different concentrations of P/A-2, 20% and 23% (w/v), respectively.

- SEM images of **20%** P/A-2:

The material shows an irregular porous internal morphology, Figure 11.

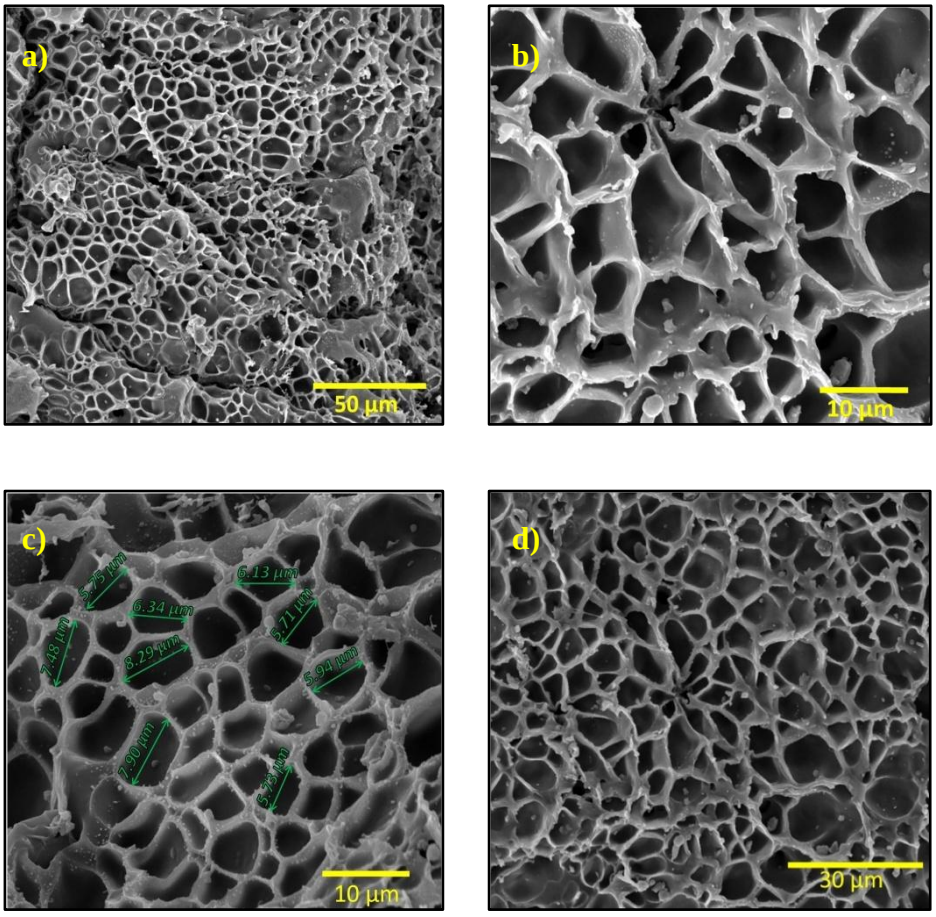


*Figure 11. Internal morphology of photopolymerized P/A-2 hydrogel, 20%. SEM images.*

The pore size goes from 4 to 12 µm, as can be appreciated in Figure 11 c).

- ω SEM images of **23%** P/A-2:

In this case, the material shows also an irregular porous internal morphology, Figure 12.

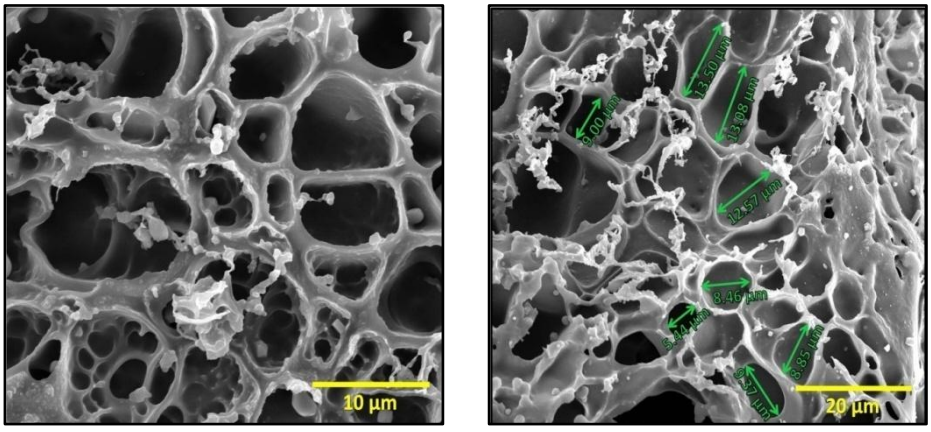


*Figure 12a. Internal morphology of photopolymerized P/A-2 hydrogel, 23%. SEM images.*

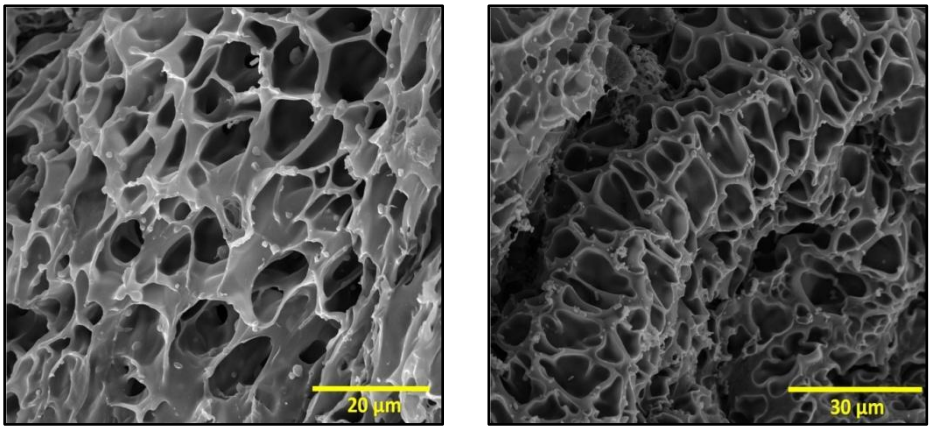


*Figure 12b. Internal morphology of photopolymerized P/A-2 hydrogel, 23%. SEM images.*

The pore size varies from 5 to 14 µm, what is quite similar to the material at 20 %(w/v).

#### 4.3.1.3.-Swelling and degradation

Scaffolds for tissue engineering applications are required to be biodegradable, and, consequently experiments to determine the extent and rate of degradation were necessaries.

The swelling and the degradation processes of the highly crosslinked material, P/A-2, were studied for both concentrations, 20 and 23 % (w/v) (see Experimental section 5.5).

The swelling, which is defined as the increase in volume of the gel, caused by the absorption of liquid from the environment, can be calculated as the weight taken at a certain time, $W_t$, divided by the initial one, $W_o$.

$$swelling\ rate\ = \frac{Wt}{Wo}$$

In this way, at the beginning of the test, the swelling rate has to be equal to 1, and when the hydrogel is completely degraded, it has to be equal to zero.

Figure 13 shows the results from the test performed for the P/A-2 photopolymerized material, at two different concentrations.

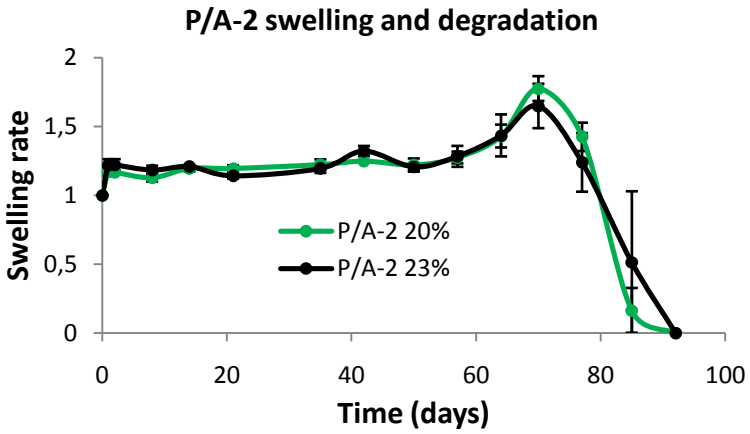


*Figure 13. Swelling and degradation profile of the P/A-2 photopolymerized hydrogel at different*

Both highly crosslinked materials show a similar behavior. Initially they present a low swelling rate. After 50 days, the swelling ratio increases faster, reaching its maximum after 70 days of experiment. This is because the bonds within the hydrogel structure are being degraded, causing loss of the structural integrity and allowing to the hydrogel absorb bigger amounts of surrounding PBS.

The swelling of the hydrogel directly affects the morphology thereof. The degradation continues until the complete breakup of the gel structure. The total time required for this compound to complete the breakup was 92 days (see Figure 14).

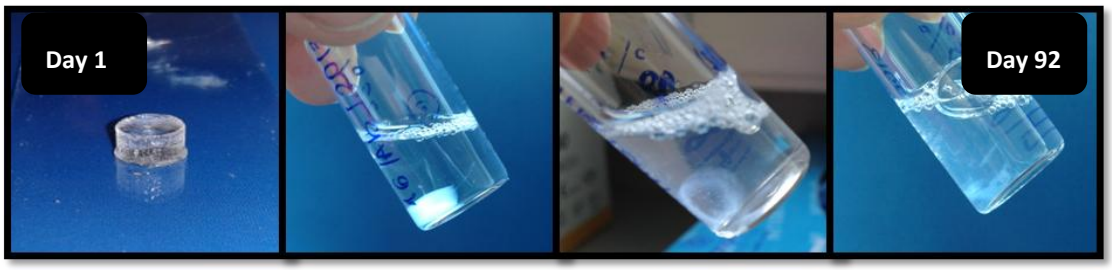


*Figure 14. Pictures from the progressive degradation of photopolymerized P/A-2 hydrogels, collected during the swelling and degradation test.*

### 4.3.2. NANOGEL (NANOSTRUCTURED HYDROGEL)

#### 4.3.2.1.-Critical micelle concentration (CMC) determination

A very important step previous to the nanogel preparation, is to know from which concentration in solution, our materials are organized into micelles.

The micelles are made by the self-assembly of amphiphiles above a certain level of concentration of this material in solution, the so called critical micelle concentration (CMC)[20,21]. In these micelles, the hydrophobic chains aggregate together to form the core and the hydrophilic chains are extended towards the aqueous environment.

For determining the CMC of P/C-2 and P/A-2 we have followed a method based on pyrene fluorescence[22]. Pyrene is a hydrophobic compound, which is encapsulated within the hydrophobic part of the micelles above the CMC of the corresponding amphiphilic compound. In this method, the changes in the ratio of pyrene excitation spectra intensities are monitored in a fluorescence spectrometer, in a range from 300 to 350 nm with a $\lambda_{em}$ = 390 nm. The ratio between the excitation intensity at 335 nm (encapsulated pyrene) and the intensity at 332 nm (non-encapsulated pyrene) can provide the information about the location of pyrene probes in the solution, and hence about the concomitant formation of the micelles

The results obtained for our materials are gathered in Figure 15.

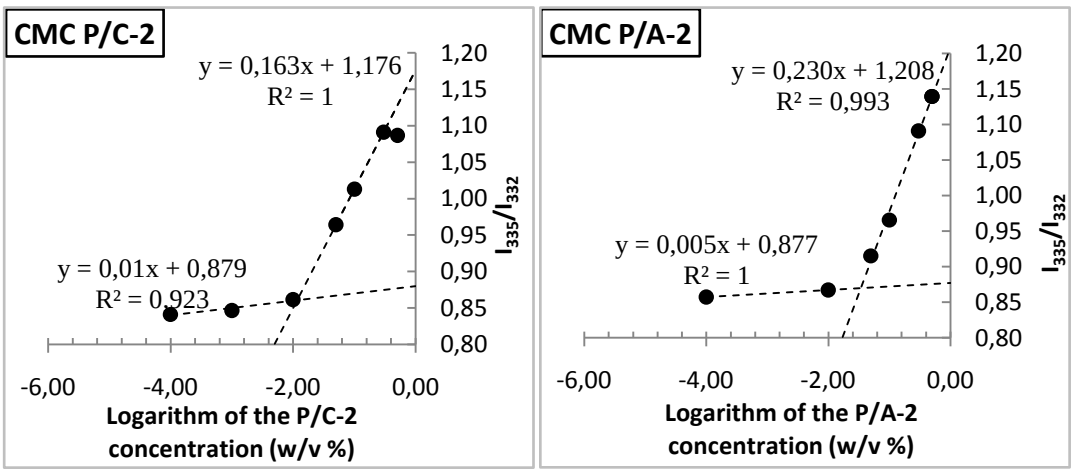


*Figure 15. Results from the pyrene method to calculate the CMC.*

From where we obtain the values of $CMC_{P/C-2}$ = 0.034 %(w/v), and $CMC_{P/A-2}$ = 0.011 %(w/v), by establishing the intersection of the straights.

These CMC are much lower than the one of the starting material, Pluronic F127, which has a CMC = 0.25 % (w/v)[20]. This significant (one order of magnitude) decrease of the CMC could minimize or overcome the problem that occurs with Pluronic, for which dissociation of the micelles upon dilution leads to the release of encapsulated drug before it reaches the targeted site.

Another important fact to underline is the lower CMC for the P/A-2 material with respect to P/C-2 material. This result proves that modifying the ending groups from hydroxyl to acrylate groups, micelle formation becomes easier, requiring lower concentration for micelles to form.

#### 4.3.2.2.-Photopolymerized nanogels

Nanogels were prepared by disolving P/A-2 in distilled water containing the photoinitiator Irgacure 2959 (see Experimental section 5.6). Then, the solution was UV-irradiated and next, the photopolymerized nanogels were dyalized during 24 hours and finally they were filtered[23]. The correct photopolymerization of the nanogels was checked by $^1$H NMR, observing that all signals corresponding to unreacted acrylate groups disappear after the photopolymerization process (Figure 16).

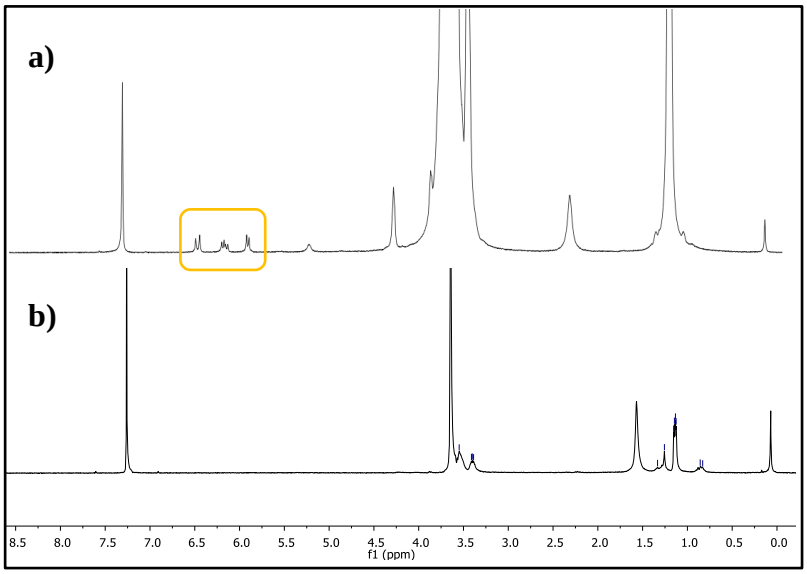


*Figure 16. $^1$H-NMR of P/A-2 material. a) original synthesized compound. b) Photopolymerized nanogel, dialyzed, filtered, lyophilized, re- dissolved in distilled water, lyophilized again and solved in $CDCl_3$.*

The photopolymerized nanogels obtained in this way, were named "PDF nanogels", what means they have been photopolymerized, dialyzed and filtered. The characteristics of these PDF nanogels where checked by SEM, TEM and DLS.

Another performed test on these nanogels was to submit the PDF nanogel to a lyophilization process, getting a solid material. This solid was mixed with distilled water to verify that its properties were maintained. Checking the characteristic of this redissolved nanogel also by TEM, SEM and DLS. The nanogels obtained in this way are named "PDF re-dis nanogels", what means they are photopolymerized, dialyzed, filtered, lyophilized and re-dissolved again. The aim of this experiment was twofold: One, to know if the material withstands manipulations for future applications in which the fact of having a solid material could represent some advantages. Second to know that micelles don't become an indissoluble aggregate block.

#### 4.3.2.3.-Morphological characterization

To characterize the morphology of the photopolymerized P/A-2 nanogel, TEM and SEM have been used.

Throught both techniques it has been proven the formation of nanostructures which can be interpreted as aggregates of micelles. The rounded shape is present for the PDF nanogel and also for the PDF re-dis nanogel, as can be perfectly appreciate in the SEM images (Figures 17, 18, 19 and 20).

- Characterization by **TEM**

**- P/A-2 PDF nanogel**

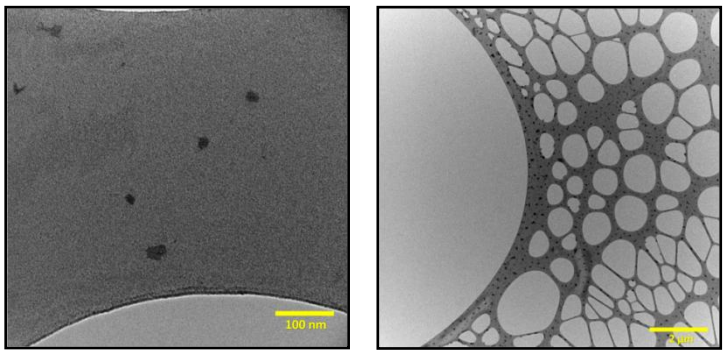


*Figure 17a. TEM images of photopolymerized, dialyzed and filtered P/A-2 nanogel.*

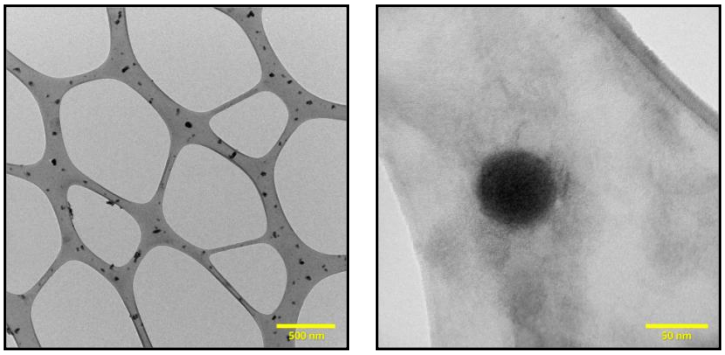


*Figure 17b. TEM images of photopolymerized, dialyzed and filtered P/A-2 nanogel.*

**- P/A-2 PDF re-dis nanogel**

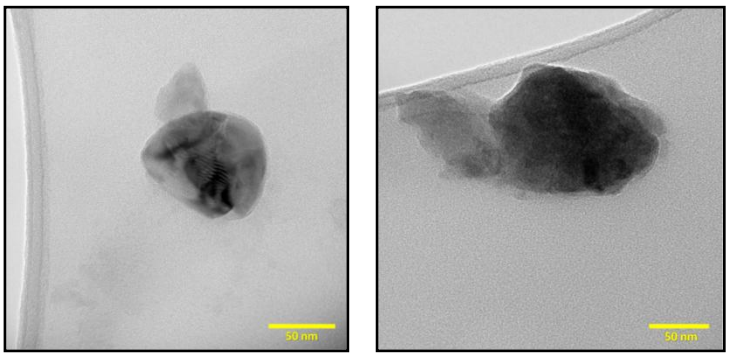


*Figure 18. TEM images of photopolymerized, dialyzed, filtered, lyophilized and redissolved P/A-2 nanogel.*

- Characterization by **SEM**

**- P/A-2 PDF nanogel**

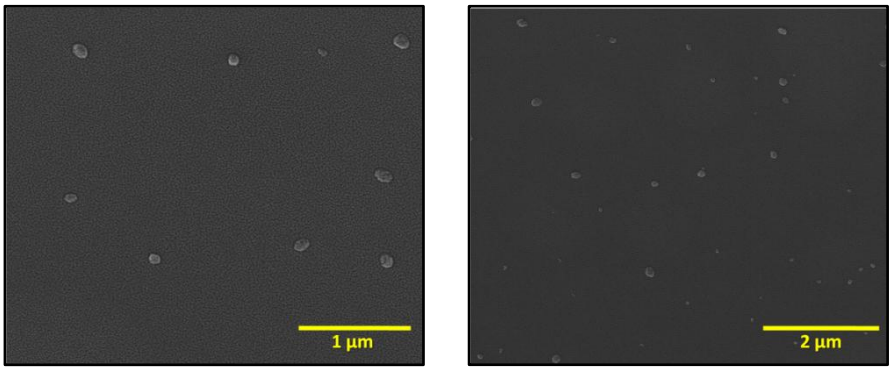


*Figure 19. SEM images of photopolymerized, dialyzed and filtered P/A-2 nanogel.*

**- P/A-2 PDF re-dis nanogel**

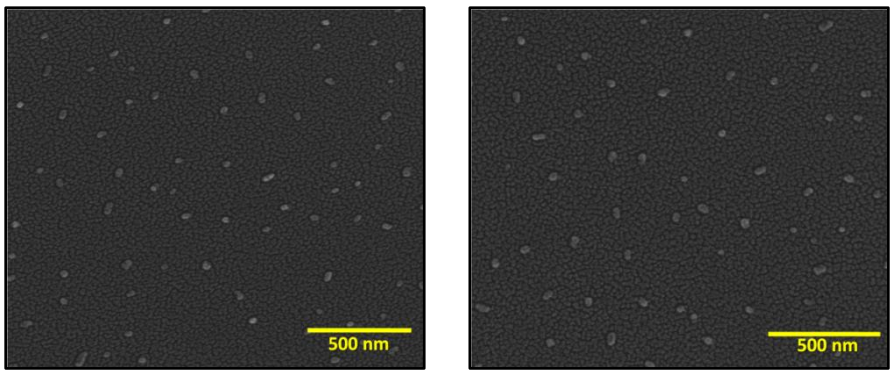


*Figure 20. SEM images of photopolymerized, dialyzed and filtered P/A-2 nanogel.*

Also, thanks to this characterization, we can confirm that the micellar aggregates don't aggregate further, once the material is lyophilized and subsequently dissolved again in distilled water.

- **Size distributions**

Results concerning the size distribution of the observed nanostructures are summarized in Table 5.

*Table 5. Summary of sizes obtained from SEM, TEM and DLS, for the P/A-2 nanogel.*

| | | **P/A-2 PDF** nanogel diameter | **P/A-2 PDF re-dissolved** nanogel diameter |
|---|---|---|---|
| **SEM** | | 52.5 -172.8 nm | 42.4- 60.8 nm |
| **TEM** (average) * | | 56.9 nm | 135.8 nm |
| **DLS** | Effective diameter | 52.0 ±1.2 nm | 83.8 ±1.0 |
| | Mean diameter | 74.9 nm | 143.9 nm |

*(* average value calculated from more than 10 structures.)*

In the case of P/A-2 PDF nanogel, the diameter obtained with different techniques results coherent, because the TEM value is within the range of SEM values, and the mean diameter obtained by DLS, is also a reasonable value, taking into account that DLS technique provides the hydrodynamic diameter.

In contrast, more divergent data are obtained in the case of P/A-2 re-dissolved nanogel. These variations can be attributed to a possible further aggregation between nanoaggregates but deeper studies should be carried out.

## 4.4.-CELL VIABILITY TESTS

Taking into account the potential biomedical applications of these materials, cell viability assays are needed.

Cell viability assays were carried out for both macroscopic hydrogels and for nanogels with two different cells types:

- Human mesenchymal stem cells (MSCs), study carried out on the macroscopic hydrogels in collaboration with Dr. María José Martinez, from Blood and Tissue Bank of Aragon.
- HeLa cells, study carried out on the nanogels in collaboration with Dr. Pilar Martín-Duque, from Araid Foundation and Rebeca González, from IIS Aragón, Biomedical Research Center of Aragon.

Concerning MSCs, the two main characteristics of these cells are[24,25]:

- Adherence to plastic. MSC must be plastic-adherent when maintained in standard culture conditions using tissue culture flasks.
- Multipotent differentiation potential. MSCs are able to differentiate into a number of mesenchymal phenotypes, including those that form bone, cartilage, muscle, fat and other connective tissues.

Concerning HeLa cells, they are a human epithelial adenocarcinoma cell line. This cell line is the oldest and most widely used human cell line[26].

### 4.4.1.MACROSCOPIC HYDROGEL

In order to check the cell viability of P, P/C-2 and P/A-2 when forming macroscopic hydrogels, tests were performed with cells MSCs.

2D and 3D experiments (Figure 21) have been performed to evaluate cell viability in the hydrogels prepared. 2D cell culture was performed by covering the cells layer with the hydrogel, while, in 3D cell culture, the hydrogel was formed in presence of the cells, then cells were distributed within the hydrogel. Cells growth and sample preparation are described in the Experimental section 5.7.

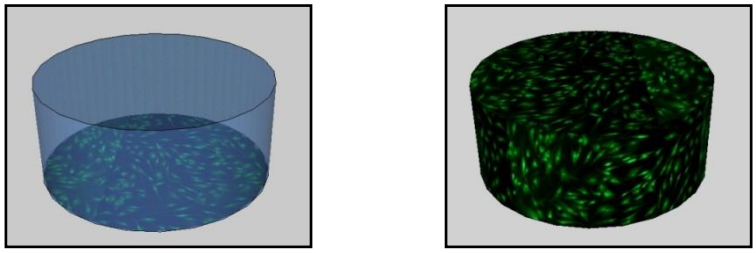


*Figure 21. Illustration of 2D and 3D cell culture*

Cell viability assays have been performed for:

- Pluronic F127, and its hydrogels, in order to compare it with our derivatives.
- Compound P/C-2, and its hydrogels.
- Compound P/A-2, and its non photopolymerized and photopolymerized hydrogels.

The assessment of cell vialibility was performed with the LIVE/DEAD® Viability/Cytotoxicity Kit, which can discriminate live from dead cells by simultaneously staining with green-fluorescent calcein-AM to indicate intracellular esterase activity and red-fluorescent ethidium homodimer-1 to indicate loss of plasma membrane integrity[27], as shown in Figure 22. (For further information, see Appendix 2.)

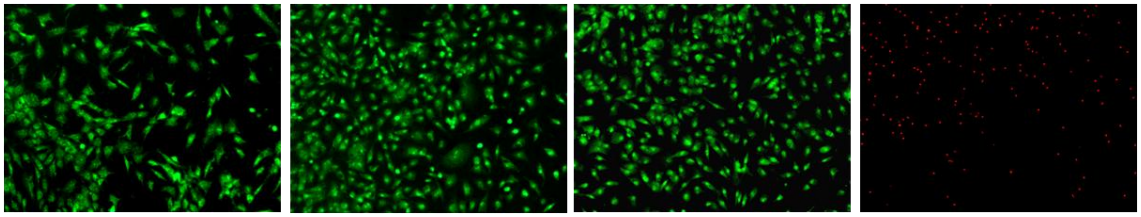

*Figure 22. Example of images taken from the fluorescence inverse microscope of stained cells with the LIVE/DEAD® KIT. Images of a)Pluronic F127, 2D, 24h, 20 %(w/v).b)P/C-2, 2D,24h, 20 %(w/v).c)P/A-2, 2D, 24h, 20 %(w/v). d)Pluronic F127, 2D, 48h, 20% wt, dead cells.*

Cell viability for the three materials was checked at 24, 48 and 72 hours by using a fluorescence inverted microscope. All experiments were performed in triplicate. In each of the three wells for each experiment, two images were taken from different areas of the well, therefore the results shown, are an average of six values.

The percentage of living cells was determined by counting living cells and dead cells, and referring to cell viability as the percentage of the amount of living cells over total present cells. All control samples, containing only cells and DMEM, presented a cell viability above the 98%.

The chosen concentrations to carry out the cell viability assays, have been the same for all tested materials:

- 5 %(w/v), 10 %(w/v). At these concentrations, none of the materials are forming the hydrogel, therefore it is considered that the monomers are in solution.
- 20 %(w/v), 23 %(w/v). Concentrations where the thermoresponsive hydrogel is formed in all materials.

#### 4.4.1.1.-Results of 2D cell viability assays.

The results obtained from the 2D cell viability assays, for Pluronic F127, P/C-2, P/A-2 and their hydrogels, are presented in Figure 23.

Figure 23 shows the variations on the cell viability depending on the material, its concentration, and time. Take notice that for these assays, the material P/A-2 was not photopolymerized.

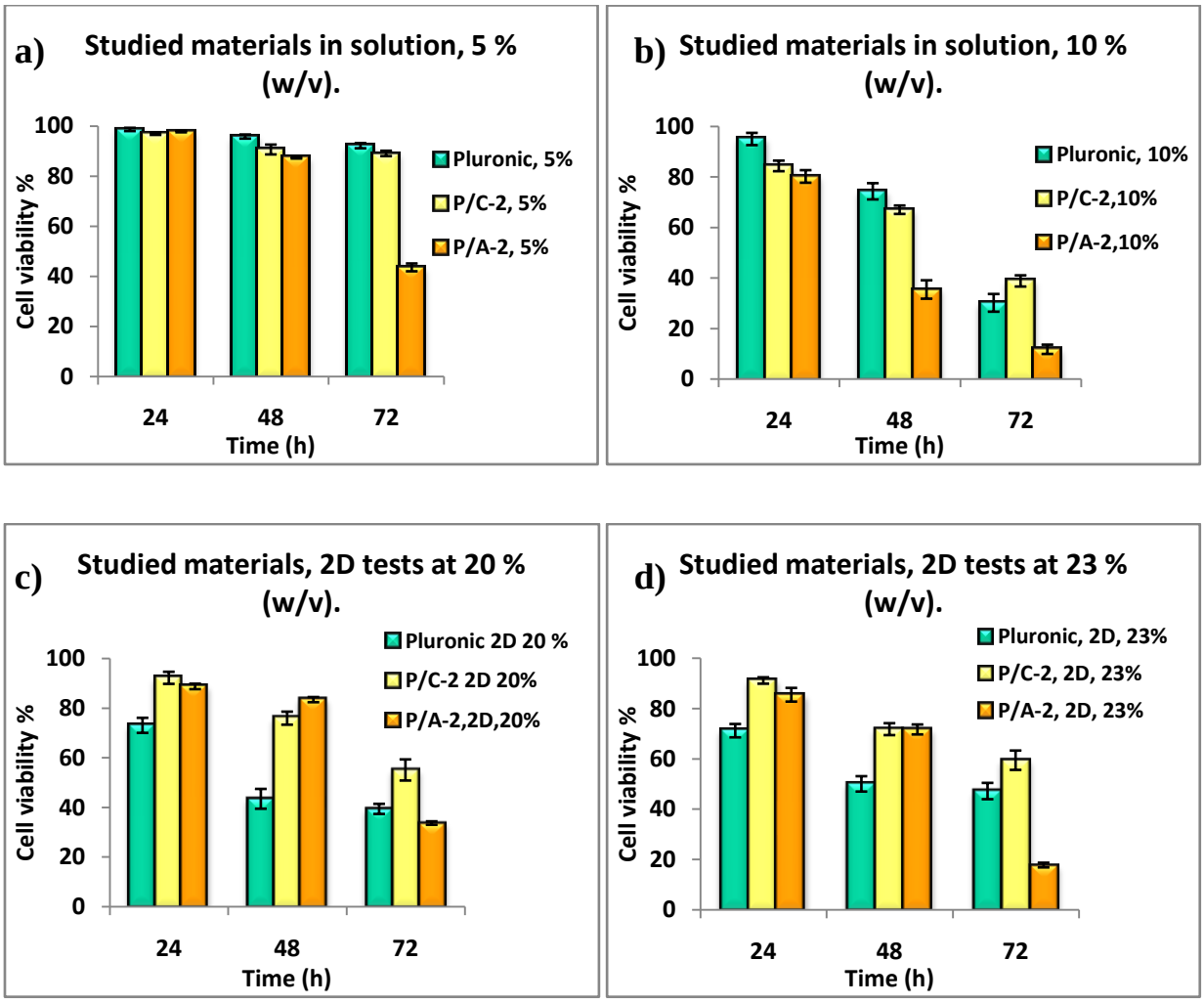


*Figure 23. Results from 2D cell viability assays at different concentrations. a)5 % (w/v), b) 10 %(w/v), c) 20 % (w/v), d)23 %(w/v).*

From these comparative studies different conclusions can be obtained:

- All materials in solution, cause a decrease in cell viability when increasing the concentration from 5 to 10%, Figure 23 a) and b). This fact is not so clearly observed when the material is forming the physical gel, comparing Figure 23 c) and d), even for some cases, the viability is higher for the higher concentration.
- In general terms, except for the material P/A-2 at 23 %, in the gel state, Figure 23 c) and d), our materials have a higher cell viability than the original Pluronic F127, showing in some cases up to 40% difference.
- The best cell viability is obtained for the material P/C-2.

#### 4.4.1.2.-Results of 3D cell viability assays.

Figure 24 shows the results obtained from the cell viability assays carried out with the same materials in a 3D system, where cells are distributed within the hydrogel network. For these assays the material P/A-2 was not photopolymerized.

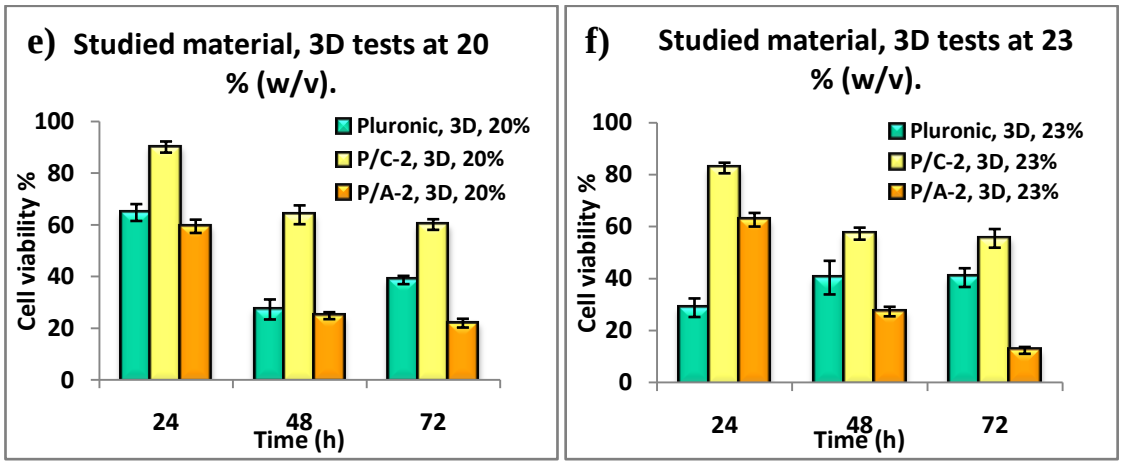


*Figure 24. Results from 3D cell viability assays at different concentrations. e) 20 % (w/v), f) 23 %(w/v).*

In this case it can not be drawn a clear conclusion about the relationship between cell vibility and concentration. What can be appreciated again, is that the best cell viability corresponds to the samples based on the material P/C-2 for both concentrations, and the worst one corresponds for those based on the acrylated material P/A-2.

Nevertheless, during measurements, it was observed for the 3D experiments that the staining providing the fluorescent green color, was much more difficult to get, and consequently, is was more difficult to quantify the alive cells in these experiments. This difficulty has been associated to a lower diffusion rate, due to the fact of working with a dye kit not originally designed for the assays in gel samples.

#### 4.4.1.3.-Non-photopolymerized *vs.* photopolymerized hydrogel. Material P/A-2.

In order to compare the difference between the material based on a physical network or on a physical-chemical network, the results obtained for the P/A-2 material at different concentrations, non-photopolymerized and photopolymerized, are presented in Figure 25.

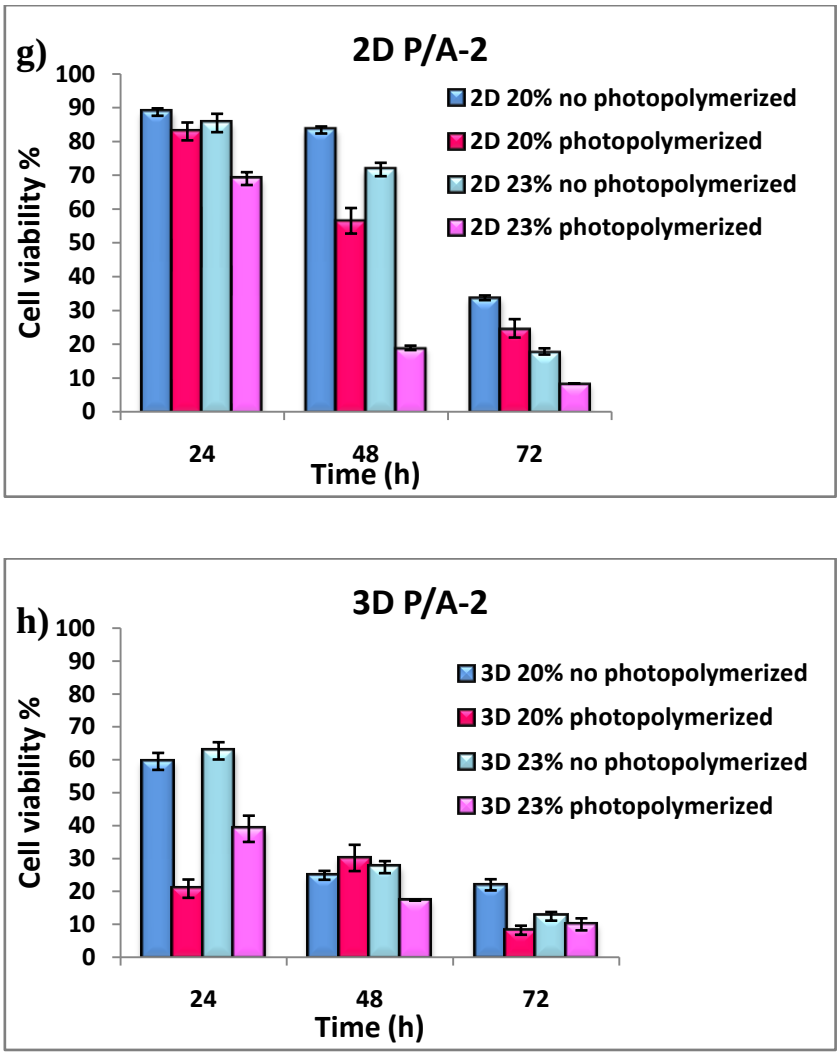


*Figure 25. Results obtained from cell viability assays. Comparison between P/A-2 material, photopolymerized and no photopolymerized, at different concentrationsin 2D and 3D assays.*

Comparing the 2D assays with 3D assays, a clear decrease in the cell viability can be appreciated concerning both concentrations and the dregree of crosslinking within the hydrogels. We have tentatively attributed these results to a limited diffusion within the polymeric network.

In almost all cases, when the material is photopolymerized, the cell viability decreases, regardless the concentration and the test type.

One possibility, to explain this result is the drowning of the cells due to the internal structure fixed by the photopolymerization process, providing an

internal network with 5–14 μm pore size distributions (see section 4.3.1.2, Morphological characterization). This fact together with the low diffusion of nutrients, may be the primary cause of cell death.

Other possibility was that UV light affects significantly cells. In order to rule out this possibility, control samples were used to test the effect of UV light applied in the photopolymerization process. In this way it was possible to check that the UV light does not affect at all cell viability, as shown in Figure 26.

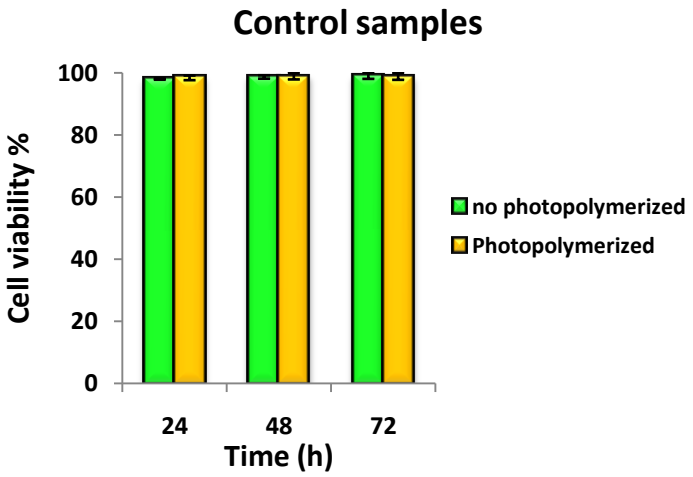


*Figure 26. UV light influence on control samples*

### 4.4.2.NANOGEL

To check the cell viability of P/A-2 acting as a nanostructured hydrogel, cell viability assays were performed with HeLa cells.

The assessment of cell viability was done with Resazurin, which is a redox dye that is commercially available as Alamar Blue®, it exhibits both colorimetric and fluorometric change that relates to cellular metabolic activity. (For further information see Appendix 2.)

Cell viability was checked at 24, 48 and 72 hours for 3 different concentrations, 0.25 mg/mL, 0.5 mg/mL and 1mg/mL. Sample preparation, is described in the Experimental

section 5.7. The cell viability is expressed as relative viability of cells (% compared to the control cells incubated only with medium).

The obtained results for this viability assay are summarized in Figure 27.

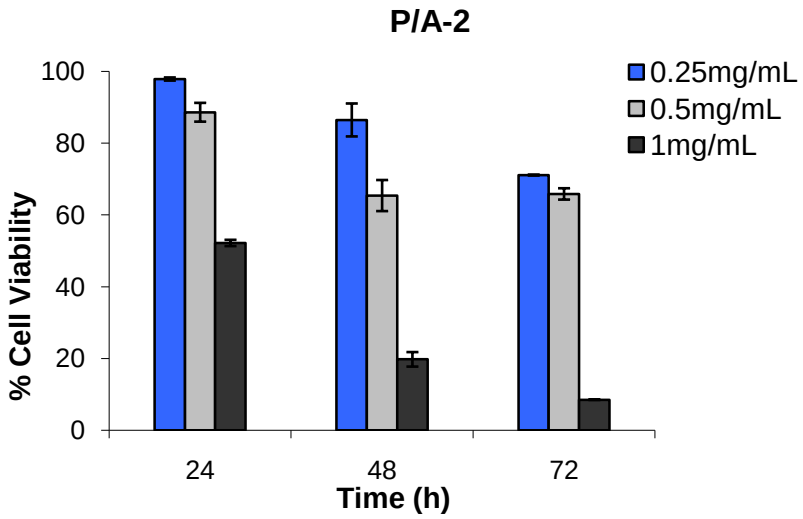


*Figure 27. Results of the cell viability test from P/A-2 PDF nanogel at different concentrations.*

As it is appreciate in Figure 27, the nanogel has a lower cell viability at higher concentrations. This fact have been associated to the idea of a possible internalization of the nanoobjects inside the cells[28].

# 5.-EXPERIMENTAL SECTION

## 5.1.-SYNTHESIS OF THE LINEAR PLURONIC DERIVATIVE

In order to obtain the linear derivative, the synthetic steps and their experimental procedure, according to Scheme 2, are the following:

**-Synthesis of P/NP-2**

The different experimental conditions used in order to obtain the P/NP-2 product, are summarized in Table 6:

*Table 6. Summary of the different experimental conditions used for the synthesis of P/NP-2*

| | | **g** | **mmol** | **eq** |
|---|---|---|---|---|
| **a** | Pluronic F127 | 5 | 0.397 | 1 |
| | *p*-nitrophenyl chloroformate | 1.128 | 5.6 | 14 |
| | DMAP | 0.684 | 5.6 | 14 |
| **b** | Pluronic F127 | 5 | 0.397 | 1 |
| | *p*-nitrophenyl chloroformate | 1.128 | 5.6 | 14 |
| | Pyridine | 0.391 | 4.94 | 12 |
| **c** | Pluronic F127 | 5 | 0.397 | 1 |
| | *p*-nitrophenyl chloroformate | 0.64 | 3.17 | 8 |
| | Pyridine | 0.391 | 4.94 | 12 |

Finally the third option, c, was the best one, due to the lower amount of p-nitrophenyl chloroformate used, and the easier processing.

-Experimental procedure with DMAP, (a).

In a flask, dry Pluronic F-127 (dried in vacuum, 115° C, 3 hours) (5g, 0.397 mmol, 1 eq) was dissolved in 15 mL of dry dichloromethane. P-nitrophenyl chloroformate (1.128 g, 5.6 mmol, 14 eq) was separately dissolved in 5 mL of dry dichloromethane and the resulting solution was added to the reaction flask under argon atmosphere. Then a solution of DMAP (4-dimethylaminopyridine) (0.684 g, 5.6 mmol, 14 eq) in 5 mL dry dichloromethane was added dropwise to the previous mixture, under argon atmosphere, appearing a white precipitate. The mixture was stirred at room temperature for 4 hours. Then, the crude was directly precipitate on 500 mL of cold diethyl ether, and placed in the fridge for one night. The solid white mixture containing the product and the subproduct was filtered, washed with cold diethyl ether and redisolved in 100 mL of dichloromethane. The organic phase was extracted twice with a 1N HCl solution (2x75 mL), and with a NaCl saturated solution (1x75 mL), dried with $MgSO_4$, filtered, and evaporated to reduce the volume. Then, the obtained oily product is precipitate in 500

mL of cold diethyl ether, placed into the fridge during one night, filtered and washed in order to obtain the product as a yellowish powder. Yield: 74 %.

-Experimental procedure with pyridine, (b and c).

In these cases two different amounts of *p*-nitrophenyl chloroformate were used.

In a flask, dry Pluronic F-127 (dried in vacuum, 115° C, 3 hours) (5g, 0.397 mmol, 1 eq) was dissolved in 15 mL of dry dichloromethane. Dry pyridine (0.4 mL, 4.94 mmol, 12 eq) was added to mixture drop by drop under argon atmosphere. *P*-nitrophenyl chloroformate (1.128 g, 5.6 mmol, 14 eq in experiment (b), or 0.64 g, 3.17 mmol, 8 eq in experiment (c)) was separately dissolved in 5 mL of dry dichloromethane and the resulting solution was added to the initial one under argon atmosphere, appearing a white precipitate. The mixture was stirred at room temperature for 24 hours. Then, the crude is redisolved with 50 mL of dichloromethane and extracted twice with a 1M $NaHSO_4$ solution (2x30 mL) and with a NaCl saturated solution (1x30 mL), dried with $MgSO_4$, filtered, and evaporated to reduce the volume. Then, the obtained oily product is precipitate in 500 mL of cold diethyl ether, placed into the fridge during one night, filtered and washed in order to obtain the product as a yellowish powder. Yield: 75 % (b), 80 % (c).

$^{1}$H-NMR (300 MHz, $CDCl_3$): δ (ppm): 1.13 (m, 201H, A), 3.39-3.80 (m, ~ 1100H, B, C, D, E, F), 4.07 (m, 4H, G), 7.37 (m, 4H, J), 8.26 (m, 4H, K).

$^{13}$C-NMR (75 MHz, $CDCl_3$): δ (ppm): 17.4- 17.5 (A), 68.4 (G), 68.7 (F), 70.7 (D, E), 72.9- 73.5 (C), 75.2- 75.4- 75.6 (B), 121.8 (J), 125.4 (K), 145.5 (L), 152.5 (H), 155.6 (I).

IR ($cm^{-1}$, ATR-FTIR): 2867 (C-H st), 1769 (C=O st carbonate), 1110 (C–O–C).

MS (MALDI+): 4999.3 m/z and 12842.8 m/z.

**-Synthesis of P/C-2**

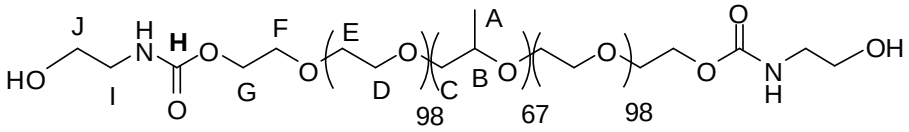


In a flask, the compound P/NP-2 (2g, 0.154 mmol, 1eq), was dissolved in dry dichloromethane, 13 mL. Ethanolamine (0.038 g, 0.622 mmol, 4 eq) was dissolved into 2 mL dichloromethane and added dropwise to the previous solution under argon atmosphere. The mixture was stirred at room temperature for 24 hours. Then, the crude was precipitate in 300 mL of cold diethyl ether and stored in the fridge overnight. The product was filtered and washed with cold diethyl ether. Yield: 80 %.

$^{1}$H-RMN (300 MHz, $CDCl_3$): δ (ppm): 1.12 (m, 201H, A), 3.30-3.80 (m, ~ 1100, B, C, D, E, F, I, J), 4.21 (m, 4H, G).

$^{13}$C-RMN (100 MHz, $CDCl_3$): δ (ppm): 17.4-17.5 (A), 43.6 (I), 61.8 (J), 63.9 (G), 68.6-68.7-69.6 (F), 70.6 (D, E), 72.9- 73.4 (C), 75.2- 75.4- 75.5 (B), 157.0 (H).

IR: ($cm^{-1}$, ATR-FTIR):1722.3 (C=O st, carbamate), 3250-3500 (O-H st).

MS (MALDI+): 5936.3 m/z and 13608.6 m/z.

**-Synthesis of P/A-2**

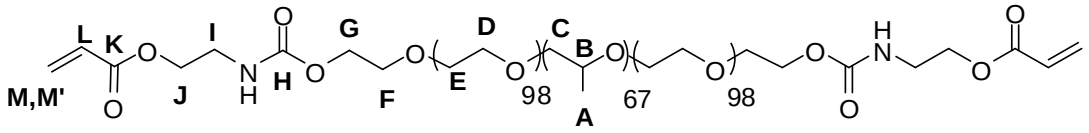


In a flask, P/C-2 (1.2 g, 0.0939 mmol, 1 eq), was dissolved in 10 mL of dry dichloromethane. 150 mg of 4-methoxyphenol were added. The flask was placed in an ice bath and triethylamine (TEA) (0.0836g, 0.826 mmol, 8.8 eq), was added dropwise under inert atmosphere. Next, acryloil chloride (0.067 g, 0.725 mmol, 8 eq) was added dropwise and also under inert atmosphere. The reaction mixture was stirred at room temperature for 24 hours in the dark. The solution was passed through a neutral alumina column and the filtrate was dried with $Na_2CO_3$ during 2 hours, filtered and evaporated

to reduce the volume. Finally the product was precipitate in 200 mL of cold diethyl ether and stored in the fridge overnight. The product was filtered and washed with cold diethyl ether. Yield: 69 %.

$^{1}$H-RMN (300 MHz, $CDCl_3$): δ (ppm): 1.12 (m, 201H, A), 3.37-3.80 (m, ~ 1100H, B, C, D, E, F, I), 4.22 (m, 8H, G,J), 5.85 (dd, $J_{cis}$=10.1 Hz, $J_{gem}$=1.2Hz, 2H, M), 6.12 (dd, $J_{trans}$= 17.3 Hz, $J_{cis}$= 10.4 Hz,2H, L), 6.41 (dd, $J_{trans}$= 17.4 Hz, $J_{gem}$=1.2 Hz, 2H, M').

$^{13}$C-RMN (75 MHz, $CDCl_3$): δ (ppm): 17.4- 17.5 (A), 39.9 (I), 63.5 (F), 66.7 (G), 68.9 (J), 70.4 (D, E), 72.8- 73.2 (B), 75.2 (C), 127.9 (L), 130.9(M), 156.2 (H), 165.7 (K).

IR: ($cm^{-1}$, ATR-FTIR):1728.1 (C=O st, carbamate)

MS (MALDI+): 5938.6 m/z and 13644 m/z.

## 5.2.-SYNTHESIS OF THE HYBRID DENDRITIC-LINEAR-DENDRITIC BLOCK COPOLYMER

**-Synthesis of Benzylidene-2,2-bis(oxymethyl)propionic acid.**

In a flask, 2,2-Bis(hydroxymethyl)-propionic acid (30 g, 223.7 mmol), benzaldehyde dimethyl acetal (56 mL, 378.1 mmol) and p-toluenesulfonic acid monohydrate (2.03 g, 10.5 mmol) were solved in 120 mL of acetone. The reaction mixture was stirred for 4 hours at room temperature. After storage of the reaction mixture in the refrigerator overnight, the solid was filtered off and washed with cold acetone to give the product as a white powder. Yield: 49 %.

$^{1}$H-RMN (300 MHz, $CDCl_3$): δ (ppm): 1.11 (s, 3H, G), 3.70 (d, *J*=11.7 Hz, 2H, F), 4.64 (d, *J*=11.4 Hz, 2H, F´), 5.49 (s, 1H, E), 7.37 (m, 3H, A, B), 7.47 (m, 2H, C).

$^{13}$C-RMN (75 MHz, $CDCl_3$): δ (ppm): 17.7 (G), 42.1 (H), 73.4 (F), 101.9 (E), 126.2 (C), 128.3 (B), 129.0 (A), 137.5 (D), 178.8 (I).

IR ($cm^{-1}$, KBr): 3005 (OH), 2865 (C-H st), 1702 (C=O).

**-Synthesis of Benzylidene-2,2-bis(oxymethyl)propionic anhydride.**

In a flask, benzylidene-2,2-bis(oxymethyl)propionic acid, (11.0 g, 49.6 mmol) and DCC (5.7 g, 27.7 mmol) were mixed in 200 mL of $CH_2Cl_2$. The reaction mixture was stirred overnight at room temperature. The precipitated urea DCC byproduct was filtered off and washed with a small volume of $CH_2Cl_2$. The crude product was concentrated using a rotavapor and precipitated into 1 l of cold hexane. After one night in the fridge, the product is filtered and washed with cold hexane to give the product as a white powder. Yield: 92 %.

$^{1}$H-RMN (300 MHz, $CDCl_3$): δ (ppm): 1.12 (s, 6H, G), 3.69 (d, *J*=11.6 Hz, 4H, F), 4.66 (d, *J*=11.7 Hz, 4H, F´), 5.47 (s, 2H, E), 7.34 (m, 6H, A, B), 7.45 (m, 4H, C).

$^{13}$C-RMN (75 MHz, $CDCl_3$): δ (ppm): 16.9 (G), 44.2 (H), 73.2 (F, F´), 102.1 (E), 126.3 (C), 128.2 (B), 129.1 (A), 137.6 (D), 169.1 (I).

IR ($cm^{-1}$, KBr): 2865 (C-H st), 1816 (C=O st sim), 1746 (C=O st as).

**-Synthesis of P/B-2**

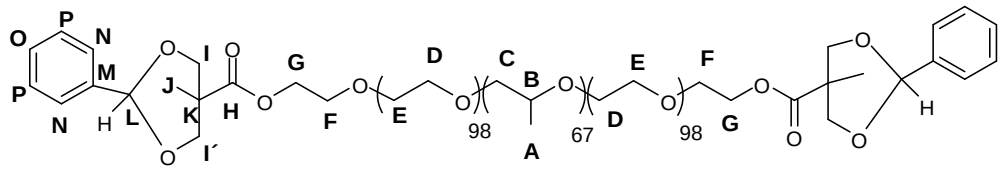

Dry Pluronic F-127 (10.0 g, 0.79 mmol), DMAP (0.12 g, 0.98 mmol) and **b**enzylidene-2,2-bis(oxymethyl)propionic anhydride (2.0 g, 4.68 mmol) were dissolved in 20 mL of $CH_2Cl_2$. The mixture was stirred at room temperature overnight under argon blanket. The excess of anhydride was quenched by adding 7 mL of methanol. The mixture was stirred while 6 hours and the crude was precipitated in 1 L of cold diethyl ether. After a night in fridge the product was isolated by filtrating and washing with diethyl ether, as a white powder. Yield: 97 %.

$^{1}$H-RMN (400 MHz, $CDCl_3$): δ (ppm): 1.04 (s, 6H, J), 1.13 (m, 201H, A), 3.37-3.82 (m, ~1100H, B, C, D, E, F, I´), 4.35 (m, 4H, G), 4.66 (d, *J*=11.6 Hz, 4H, I), 5.44 (s, 2H, L), 7.32 (m, 6H, P, O), 7.42 (m, 4H, N).

$^{13}$C-RMN (300 MHz, $CDCl_3$): δ (ppm): 17.3, 17.4 (A), 17.9 (J), 42.4 (K), 64.2 (G), 68.5- 68.6-69.1 (F), 70.5 (D, E), 72.9- 73.3 (C, I, I´), 75.1- 75.3- 75.5 (B), 101.7 (L), 126.2 (N), 128.2 (Q), 128.9 (P), 137.9 (M), 173.9 (H).

**-Synthesis of P/OH-4**

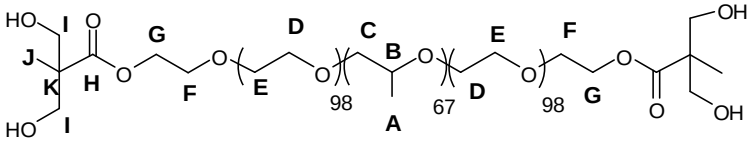

In a flask, compound P/B-2 (10 g, 0.77 mmol) was dissolved in 200 mL of EtOAc. Once P/B-2 is dissolved, 10 % (w/w) Pd/C was added. After three vacuum-argon cycles, the reaction mixture was stirred at room temperature in hydrogen atmosphere

overnight. The Pd/C was filtered off with Celite® and the filtrate was evaporated to give the product as white solid. Yield: 93 %.

$^{1}$H-RMN (400 MHz, $CDCl_3$): δ (ppm): 1.11 (s, 6H, J), 1.13 (m, 201H, A), 3.37-3.82 (m, ~1100H, B, C, D, E, F, I), 4.34 (m, 4H, G).

$^{13}$C-RMN (300 MHz, $CDCl_3$): δ (ppm): 17.1 (J), 17.3- 17.4 (A), 49.5 (K), 63.2 (G), 67.3 (I), 68.4- 68.5- 68.7 (F), 70.5 (D, E), 72.9- 73.3 (C), 75.1- 75.3- 75.5 (B), 175.6 (H).

**-Synthesis of P/NP-4**

In a flask, P/OH-4 (3 g, 0.233 mmol, 1 eq) was dissolved in 20 mL of dry $CH_2Cl_2$, then, 0.8 mL of dry pyridine and *p*-nitrophenyl chloroformate (0.75 g, 3.76 mmol, 16 eq), were added to the reaction flask under argon blanket and stirring. The reaction mixture was stirred at room temperature for 24 h. The crude was redisolved with 50 mL of dichloromethane and extracted twice with a 1M $NaHSO_4$ solution (2x30 mL) and with a NaCl saturated solution (1x30 mL), dried with $MgSO_4$, filtered, and evaporated in rotavapor to reduce the volume. Then, the product was precipitate in 300 mL of cold diethyl ether, placed in the fridge overnight, filtered and washed with cold diethyl ether. Yield: 79 %.

$^{1}$H-RMN (300 MHz, $CDCl_3$): δ (ppm): 1.13 (m, 201H, A), 1.38 (s, 6H, J), 3.37-3.85 (m, ~1100H, B, C, D, E, F), 4.34 (m, 4H, G), 4.47 (d, *J*= 9 Hz, 4H, I), 4.58 (d, *J*= 9 Hz, 4H, I´), 7.37 (m, 8H, M), 8.26 (m, 8H, O).

$^{13}$C-RMN (75 MHz, $CDCl_3$): δ (ppm): 17.4- 17.5 (A), 17.7 (J), 46.5 (K), 64.5 (G), 68.6-68.7-69.2 (F), 70.7 (D, E, I, I´), 72.9- 73.5 (C), 75.2- 75.4- 75.6 (B), 121.7 (M), 125.3 (O), 145.5 (P), 152.1 (L), 155.2 (N), 171.5 (H).

**-Synthesis of P/C-4**

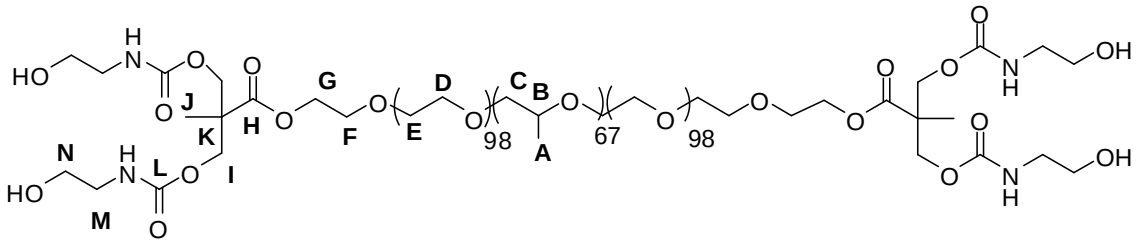

In a flask, P/NP-4 (1.6 g, 0.118 mmol, 1 eq) was dissolved in 10 mL dry dichloromethane under argon blanket and stirring. Ethanolamine (0.043g, 0.704 mmol, 6 eq) along with 2 mL of dry dichloromethane, were added to the reaction flask. The reaction mixture was stirred for 24 h at room temperature, next, the crude was precipitated into 200 mL of cold diethyl ether and placed in the fridge overnight. The product was filtered and washed with cold diethyl ether to obtain the product as a white powder. Yield: 90 %.

$^{1}$H-RMN (300 MHz, $CDCl_3$): δ (ppm): 1.13 (m, 201H, A), 1.23 (s, 6H, J), 3.29 (m, 8H, M), 3.39-3.87 (m, ~1100H, B, C, D, E, F, N), 4.26 (m, 12H, I, G).

$^{13}$C-RMN (75 MHz, $CDCl_3$): δ (ppm): 17.1 (A), 43.3 (K), 46.4 (M), 61.2 (N), 65.6 (I) 66.8 (G), 68.6 (F), 70.2 (D, E), 72.6- 73.08 (C), 74.8- 75.2 (B), 156.35 (L), 172.85 (H).

**-Synthesis of P/A-4**

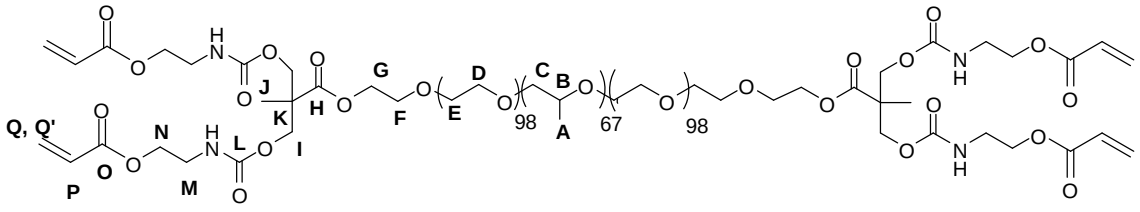

In a flask, P/C-4 (1.2 g, 0.091 mmol, 1 eq) was solved in 10 mL of dry dichloromethane (or dry THF) under argon blanket and stirring, then the inhibitor, 4-methoxyphenol was added in excess (300-850 mg). Once the mixture was solved, the flask was placed in an ice bath and TEA (0.162 g, 1.6 mmol, 17.6 eq) was added dropwise under inert atmosphere. Next, acryloil chloride (0.132 g, 1.46 mmol, 16 eq) was added dropwise and also under inert atmosphere. The reaction mixture was stirred at room temperature

for 48 hours in the dark. The solution was passed through a neutral alumina column and the filtrate was dried with $Na_2CO_3$ during 2 hours, filtered and evaporated to reduce the volume. Finally the product was precipitate in cold diethyl ether (200-300 mL) and stored in the fridge overnight. The product was filtered and washed with cold diethyl ether.

## 5.3.-TIM and DSC procedures

- TIM procedure

First, the chosen concentration samples were prepared in solution with PBS (10 mM, pH =7.4), 100 µl, inside a 2 mL vial. To obtain a good solution the samples were placed at 4 º C overnight and in the dark.

Then, the samples were heated with a heater block (speed 1 ºC/min.).

During the heating process, the state of the samples was visually followed to determine at what temperature, indicated by the heater block, the transition from sol state to gel state took place for each sample. The LCST was defined as the temperature when the material does not flow for at least 10 seconds, when the vial is upside down.

- DSC procedure

The samples were introduced inside of airtight capsules, and the applied method for all samples was the same: to heat the sample from -10 °C to 50 °C, following by a cooling process from 50 °C to -10 °C with a ramp of 5 °C/min.

## 5.4.-Photopolymerized macroscopic hydrogel obtention

To prepare the photopolymerized hydrogels, the obtained products were prepared at selected concentrations, by dissolving them in 100 µL of a previously prepared PBS 10 mM solution containing 0.1% w/v of photoinitiator Irgacure 2959.

> IRGACURE 2959 is a highly efficient non yellowing radical photoinitiator for the UV curing of systems comprising of unsaturated monomers and prepolymers. It is especially suited where low odor is required and for use in water borne systems based on acrylate or unsaturated polyester resins[29].

These solutions were stored overnight at 4°C and in darkness to ensure a good and homogeneous dissolution of the products.

Subsequently, the gels are formed by the effect of temperature. To do this, a hotplate was used (see Figure 28). Upon the hotplate, a cylindrical holder of 6 mm diameter by 3 mm high, is positioned on a glass slide.

When the achieved temperature by the hotplate was 37°C, the cold solution prepared is poured into the holder. This process must be carried out keeping and manipulating the samples in cold conditions, in order to prevent the gel formation prematurely.

Once the gel was formed within the holder, it was exposed to ultraviolet radiation (365nm) at 8 cm distance for 10 minutes to fix the structure.

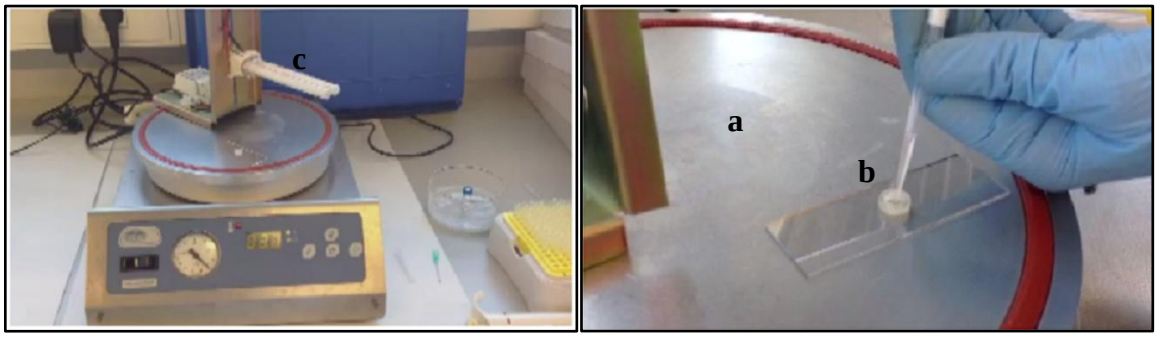


*Figure 28. Hydrogel's photopolymerization system. a) hotplate at 37 ºC. b) cylindrical mould. c) UV lamp.*

After the 10 minutes of exposure to the UV light, the photopolymerized hydrogels are demoulded and used for its morphological characterization by SEM and for the degradation studies.

## 5.5.-Swelling and degradation procedure

The procedure method was as follows:

- To weigh the freshly prepared photopolymerized hydrogel at certain concentration. Defining $W_o$ as the initial weight of the hydrogel.
- Each sample was incubated in 2mL of PBS (10 mM, pH=7.4) at 37 °C.
- At constant intervals of time, equal for all samples, each one was weighed. For this purpose, the sample was dried prior to weighing by removing excess of

PBS, subsequently, another 2 mL of new PBS in the same conditions were added to recover the experimental swelling conditions.

## 5.6.-Photopolymerized nanogel obtention.

For obtaining the nanogels, two solutions were prepared separately

- First, it is necessary to prepare a solution containing 0.1% (w/v) of the photoinitiator Irgacure 2959 in distilled water. (Solution A)
- Secondly, a solution containing the product P/A-2, 10 % in (w/v), dissolved in 600 µL of solution A, this one was placed overnight at 4ºC in darkness to ensure an homogeneous dissolution of the material. (Solution B)

Then, both solutions were filtered with a 0.20 µm filter, and taken to a final volume of 5 ml (Solution C), where the P/A-2 concentration was 0.77 % wt.

Then, the solution C was poured in a clean glass container where the photopolymerization process will be carried out.

The solution was exposed to ultraviolet radiation (365nm) with 8 cm distance between the lamp and the sample, for 10 minutes, at room temperature.

Once the structure of the nanogel has been fixed, the photopoymerized solution is placed inside a membrane [cellulose ester (CE), MWCO300 000 with a nominal pore size of 35 nm], and dialyzed for 24h at 4ºC in a 2 L vessel.

The aim of the dialysis process is to purify the nanogel, mainly by eliminating all the possible particles which could be within the nanogel solution, chiefly the presence of free monomers.

Once the dialysis process was finished, the samples are again filtered with a single use 0.20 µm filter and prepared to be characterized by TEM, SEM and DLS.

## 5.7.-MSCs and HeLa cell culture and sample preparation.

- MSCs

First MSCs were grown in alfa-MEM (minimum essential medium) with FGF (fibroblast growth factor) and 10 % of FBS (fetal bovine serum). Media was removed each 3 or 4 days, and cells were cells trypsinized after reaching 80% confluence.

To prepare the samples, Pluronic F127, P/C-2 or P/A-2, in its solid state, were sterilized by UV light for an hour. Next, these sterilized compounds were dissolved in an also sterilized DMEM, with or without photoinitiator Irgacure 2959 (0.1 %). DMEM is a modification of Basal Medium Eagle (BME) that contains a four-fold higher concentration of amino acids and vitamins, as well as additional supplementary components.To ensure a good solubilization, samples were left overnight in the refrigerator at 4 ° C, tightly closed.

For 2D assays, 10000 cells/well were seeded in a 96 well-plate. Cells were covered by 100µL of polymeric solution (Pluronic 127, P/C-2 or P/A-2), and incubated for 5 minutes at 37 °C to reach the physical hydrogel. Then, the photopolymerization process was carried out when needed, by exposing the 96well-plate to UV light for 10 minutes at 8 cm distance. After it, 100 µL of freshly medium was added.

In the case of 3D assays, the process was similar but previously, cells were dispersed into the polymeric solution, and then the assembly was transferred to the 96 well-plate.

- *HeLa* cells

*HeLa* cells were seeded at a density of 1-3 x$10^3$ cells/well in a 96 well-plate with DMEM. The P/A-2 PDF nanogel, in this case, was prepared as explained in Experimental section 5.6, then lyophilized and dissolved again in sterile DMEM, 1mg/mL.

Upon 24h incubation, media was removed and fresh media was added to the control wells and the P/A-2 nanogel diluted in media at different concentrations (0.25, 0.5 and 1 mg/mL) was added to the rest of the wells.

Media was removed after 24, 48 and 72h of incubation with the P/A-2 PDF nanogel, and fresh media was added to all the wells (control and sample wells); then a 10% of the media volume of Alamar Blue solution (Invitrogen by Life Technologies, Thermo Fisher Scientific, Spain) was added. After 2h incubation at 37ºC, fluorescence was read at 530/590 (excitation/emission) on a Synergy HT (BioTek, USA) plate reader.

## 6.-Conclusions

- Pluronic F127 allows to prepare thermosensitive and photopolymerizable hydrogels by the incorporation of hydroxyl and acrilate terminal groups.
- The photopolymerization technique can be successfully applied for the preparation of both the macroscopic molded hydrogels and nanostructured hydrogels (nanogels).
- Concerning the macroscopic hydrogel:
    - The internal morphology, characterized by SEM, reveals a pore size distribution from 4 to 12 μm.
    - The materials exhibit a total degradation in 92 days.
    - Functionalized derivatives offer better cell viability than Pluronic F127 in the 2D assays.
- Concerning the nanostructured hydrogel:
    - Functionalized derivatives offer improved CMC than Pluronic F127.
    - The morphological characterization by TEM and SEM, have confirmed the micellar structure of the nanogels in water, and the possibility of its drying and further re-dissolution.

## 7.-References


1. Hoffman, A. S., Hydrogels for biomedical applications. *Advanced Drug Delivery Reviews* **2012,** *64*, 18-23.

2. Nguyen, K. T.; West, J. L., Photopolymerizable hydrogels for tissue engineering applications. *Biomaterials* **2002,** *23* (22), 4307-4314.

3. L. Klouda, A.G. Mikos, Thermoresponsive hydrogels in biomedical applications, European Journal of pharmaceutics and biopharmaceutics 68, **2008**, 34-45.

4. Moon, H. J.; Ko, D. Y.; Park, M. H.; Joo, M. K.; Jeong, B., Temperature-responsive compounds as in situ gelling biomedical materials. *Chemical Society Reviews* **2012,** *41* (14), 4860-4883.

5. Manuela Di Biase, P. d. L., Valeria Castelleto; Nicola tirelli, Photopolymerization of Pluronic F-127 diacrylate, a colloid template polymerization. *Soft Matter* **2011,** *7*, 4928-4937.

6. Y. Ma, Y. Tang, N.C. Billingham, S.P. Armes, *Biomacromolecules* 4 , **2003,** 864 .

7. L.Yang, P.Alexandridis, *Langmuir* 16, **2000**, 4819.

8. a) B. Jeong, Y. H. Bae and S. W. Kim, *Macromolecules*, **1999**, 32,7064–7069. b) R. Rathi, G. Zentner and B. Jeong, US Pat., 6117949, 2000. c)A. Chenite, C. Chaput, D. Wang, C. Combes, M. D. Buschmann, C. D. Hoemann, J. C. Leroux, B. L. Atkinson, F. Binette and A. Selmani, *Biomaterials*, **2000**, 21, 2155–2161. d) B. H. Lee, Y.M. Lee, Y. S. Sohn and S. C. Song, *Macromolecules*, **2002**, 35, 3876–3879.

9. Li, Y.; Rodrigues, J.; Tomas, H., Injectable and biodegradable hydrogels: gelation, biodegradation and biomedical applications. Che*mical Society Reviews* ***2012,*** 41 *(6*).

10. (a) Balakrishnan, B.; Banerjee, R., Biopolymer-Based Hydrogels for Cartilage Tissue Engineering. Che*mical Reviews* ***2011,*** 111 *(8*), 4453-4474; (b) Naveena, N.; Venugopal, J.; Rajeswari, R.; Sundarrajan, S.; Sridhar, R.; Shayanti, M.; Narayanan, S.; Ramakrishna, S., Biomimetic composites and stem cells interaction for bone and cartilage tissue regeneration. Jou*rnal of Materials Chemistry* ***2012,*** 22 *(1*2).

11. Center for Disease Control and Prevention, statistics data, **2003**. National Health Interview Survey (NHIS) Statistics.

12. T.Furukawa, D.R. Eyre and M.J. Glimcher, J. Bone Joint. Surg. Am., **1980**, 62, 79-89.

13. Khandare, J.; Calderon, M.; Dagia, N. M.; Haag, R., Multifunctional dendritic polymers in nanomedicine: opportunities and challenges. Che*mical Society Reviews* ***2012,*** 41 *(7*), 2824-2848.

14. Kabanov, A. V.; Vinogradov, S. V., Nanogels as Pharmaceutical Carriers: Finite Networks of Infinite Capabilities. Ang*ewandte Chemie-International Edition* ***2009,*** 48 *(3*0), 5418-5429.

15. Lee, W.-C.; Li, Y.-C.; Chu, I. M., Amphiphilic Poly(D,L-lactic acid)/Poly(ethylene glycol)/Poly(D,L-lactic acid) Nanogels for Controlled Release of Hydrophobic Drugs. Mac*romolecular Bioscience* ***2006,*** 6 (*1*0), 846-854.

16. G.Yu, X. Yan, C.Han, F.Huang. Characterization of supramolecular gels. *Chem.Soc.rev*.,**2013**, 42, 6697.

17. Nie, S. F.; Hsiao, W. L. W.; Pan, W. S.; Yang, Z. J., Thermoreversible Pluronic (R) F127-based hydrogel containing liposomes for the controlled delivery of paclitaxel: in vitro drug release, cell cytotoxicity, and uptake studies. *Int. J. Nanomed.* **2011,** 6, *1*51-166.

18. Cabana, A.; Aït-Kadi, A.; Juhász, J., Study of the Gelation Process of Polyethylene Oxidea–Polypropylene Oxideb–Polyethylene OxideaCopolymer (Poloxamer 407) Aqueous Solutions. Jou*rnal of Colloid and Interface Science* ***1997,*** 190 *(2*), 307-312.

19. Weiss, R.G.T., P, Molecular Gels. *Springer* **2006,** Dordrecht.

20. a) M.Hamidi, M.A. Shahbazi, K. Rostamizadeh. Copolymers: efficient carriers for intelligent nanoparticulate drug targeting and gene theraphy. *Macromol.Biosci*. **2012,** 12, 144-164.

21. Q.Gao, Q.Liang, F.Yu, J.Xu, Q.Zhao, B.Sun. Synthesis and characterization of novel amphiphilic copolymer stearic acid-coupled F127 nanoparticles for nano-technology based drug delivery system. *Colloids and Surfaces B: Biointerface*s, 88, **2011**, 741- 748.

22. Ashjari, M.; Khoee, S.; Mahdavian, A. R.; Rahmatolahzadeh, R., Self-assembled nanomicelles using PLGA-PEG amphiphilic block copolymer for insulin delivery: a physicochemical investigation and determination of CMC values. Jou*rnal of Materials Science-Materials in Medicine* **2012, 23** *(4*), 943-953.

23. Choi, W. I.; Tae, G.; Kim, Y. H., One pot, single phase synthesis of thermo-sensitive nano-carriers by photo-crosslinking of a diacrylated pluronic. *Journal of Materials Chemistry* **2008, 18** *(2*4), 2769-2774.

24. M. Dominici et al.. Minimal criteria for defining multipotent mesenchymal stromal cells. The International Society for Cellular Therapy position statement. *Cytotherapy* **(2006)** Vol. 8, No. 4, 313-317.

25. Caplan, A. I., Why are MSCs therapeutic? New data: new insight. *The Journal of Pathology* **2009, 217** (*2),* 318-324.

26. National Center for Biotechnology Information, db GaP database.

27. Invitrogen official webpage.

28. Choi, J. H.; Jang, J. Y.; Joung, Y. K.; Kwon, M. H.; Park, K. D., Intracellular delivery and anti-cancer effect of self-assembled heparin-Pluronic nanogels with RNase A. *Journal of Controlled Release* **2010***,* 147 (*3),* 420-427.

29. Bahney, C. S.; Lujan, T. J.; Hsu, C. W.; Bottlang, M.; West, J. L.; Johnstone, B., VISIBLE LIGHT PHOTOINITIATION OF MESENCHYMAL STEM CELL-LADEN BIORESPONSIVE HYDROGELS. *European Cells & Materials* **2011***,* 22, 43-55.

I would like to thank for the opportunity to perform this Final Master Work, to the research group Liquid Crystals and Polymers, to the ICMA, and also to the INA for the provided infrastructure.

At a personal level I would like to say thanks to my directors, María Blanca Ros y Teresa Sierra, for its help and for trusting me, and also thanks to Isabel Jiménez, for all she has teached me, and for her patience.

# APPENDIX 1

## φ Pluronic F-127

**$^{1}$H-NMR**

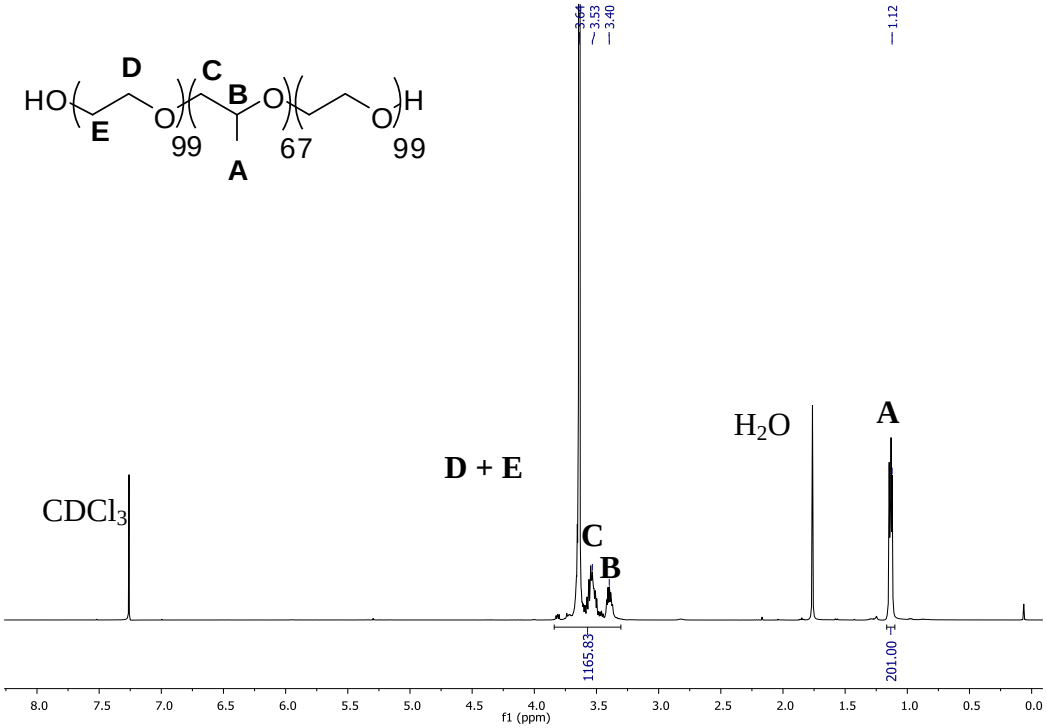


**$^{13}$C-NMR; APT**

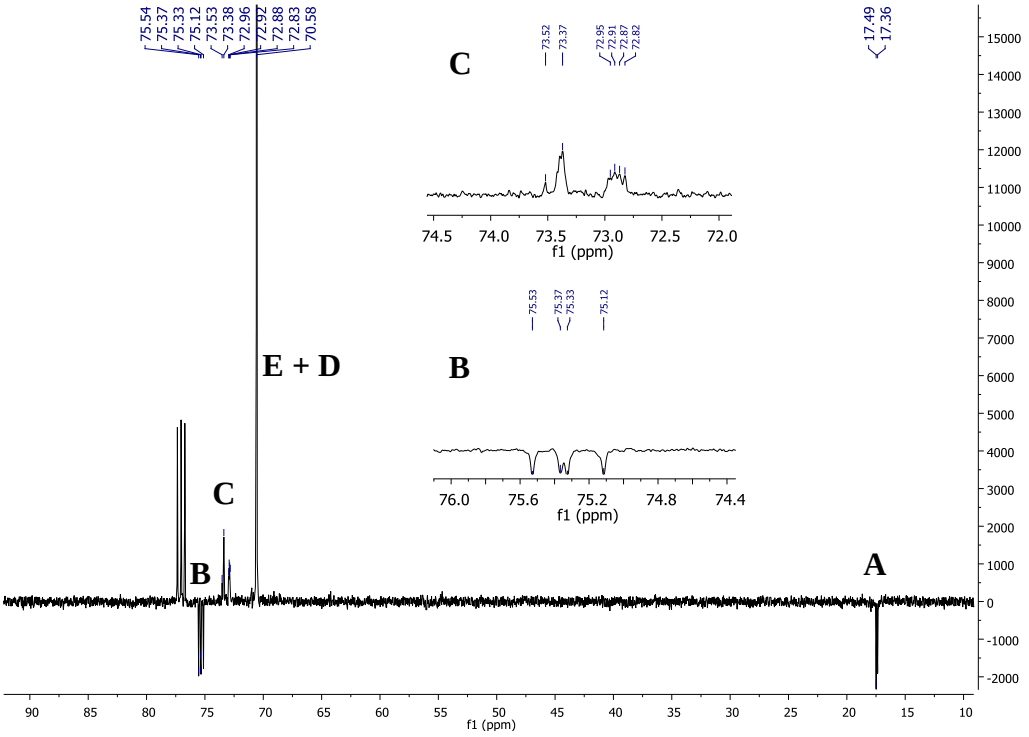

**IR**

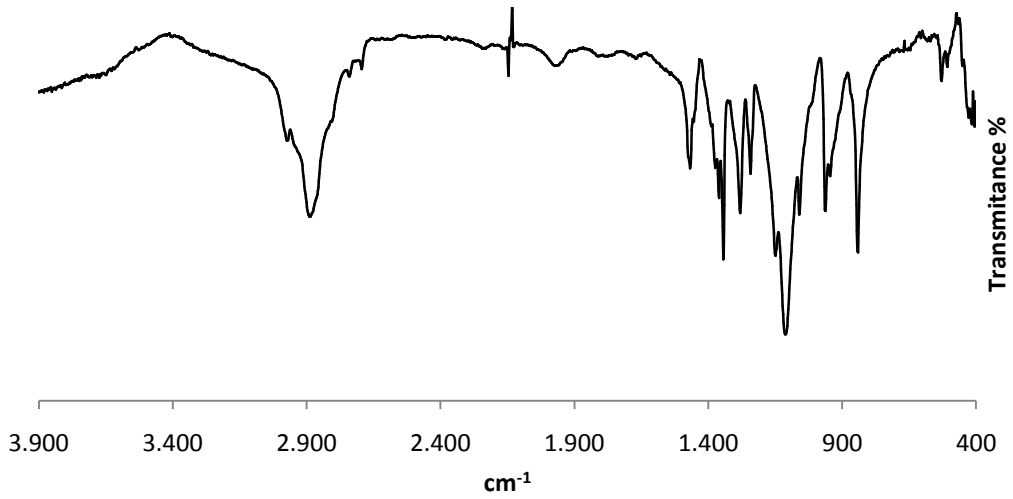
Transmitance %
3.900
3.400
2.900
2.400
1.900
1.400
900
400
cm-1

**GPC**

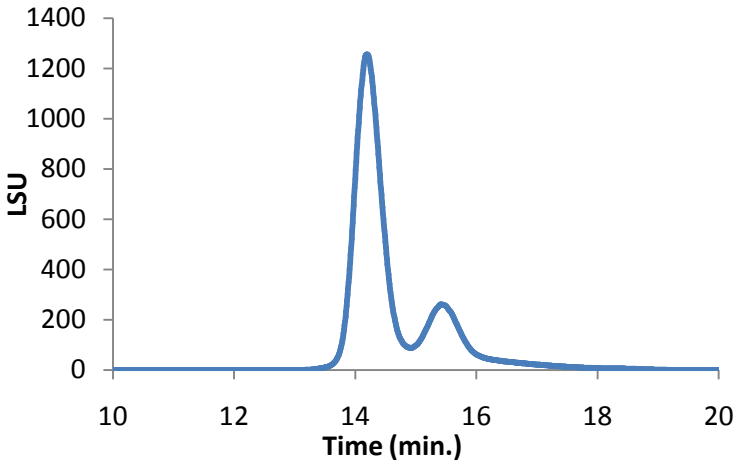
1400
1200
1000
800
600
400
200
0
LSU
10
12
14
16
18
20
Time (min.)

## φ P/C-2

### $^{1}$H-NMR

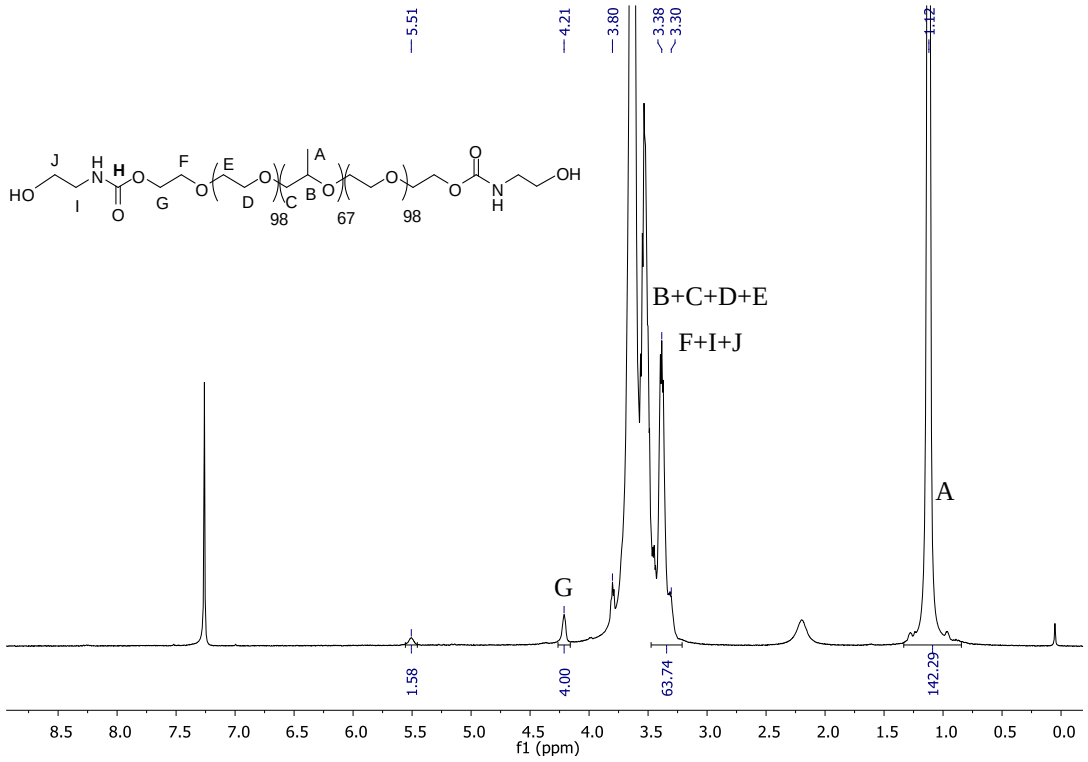


### $^{13}$C-NMR

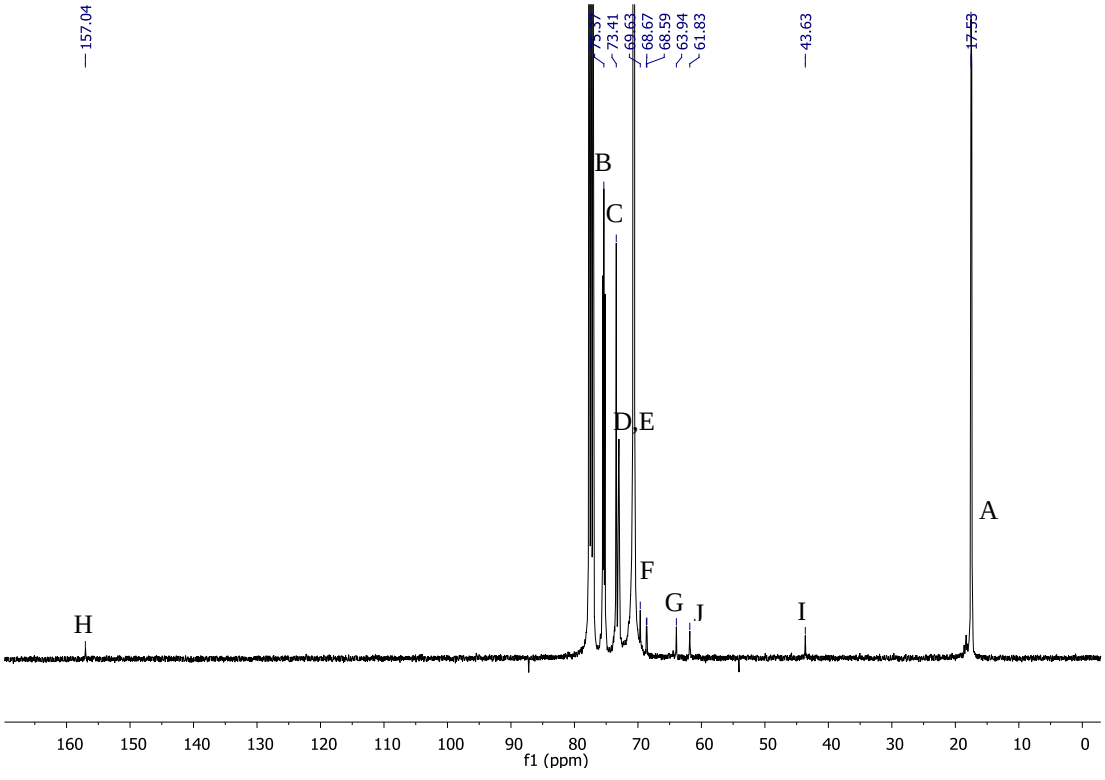

**IR**

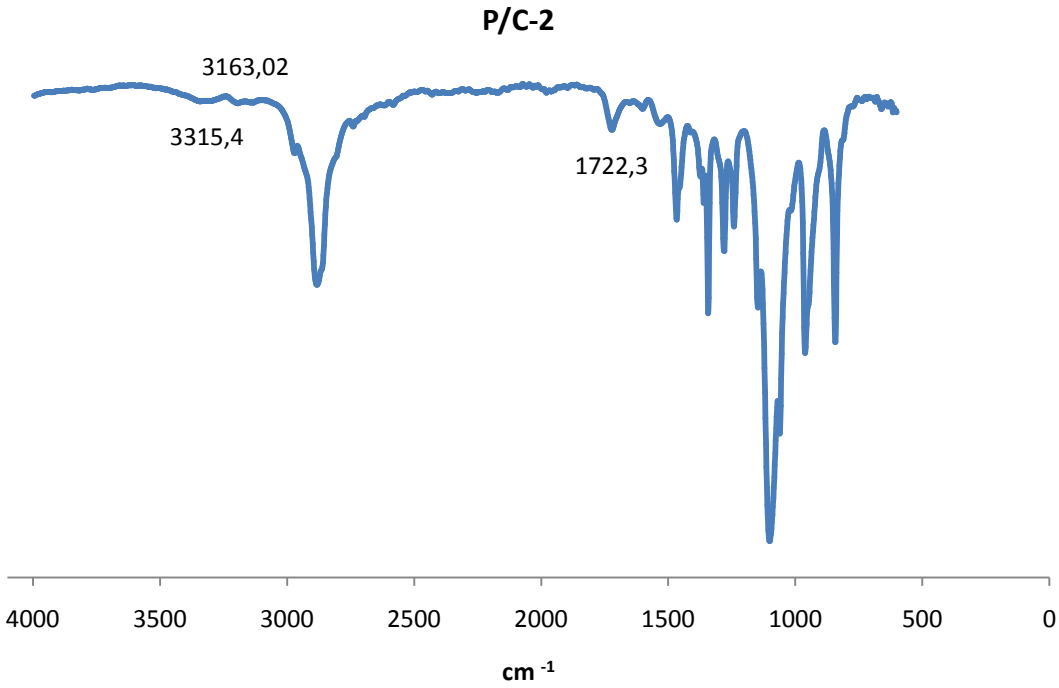


## φ P/A-2

**$^{1}$H-NMR**

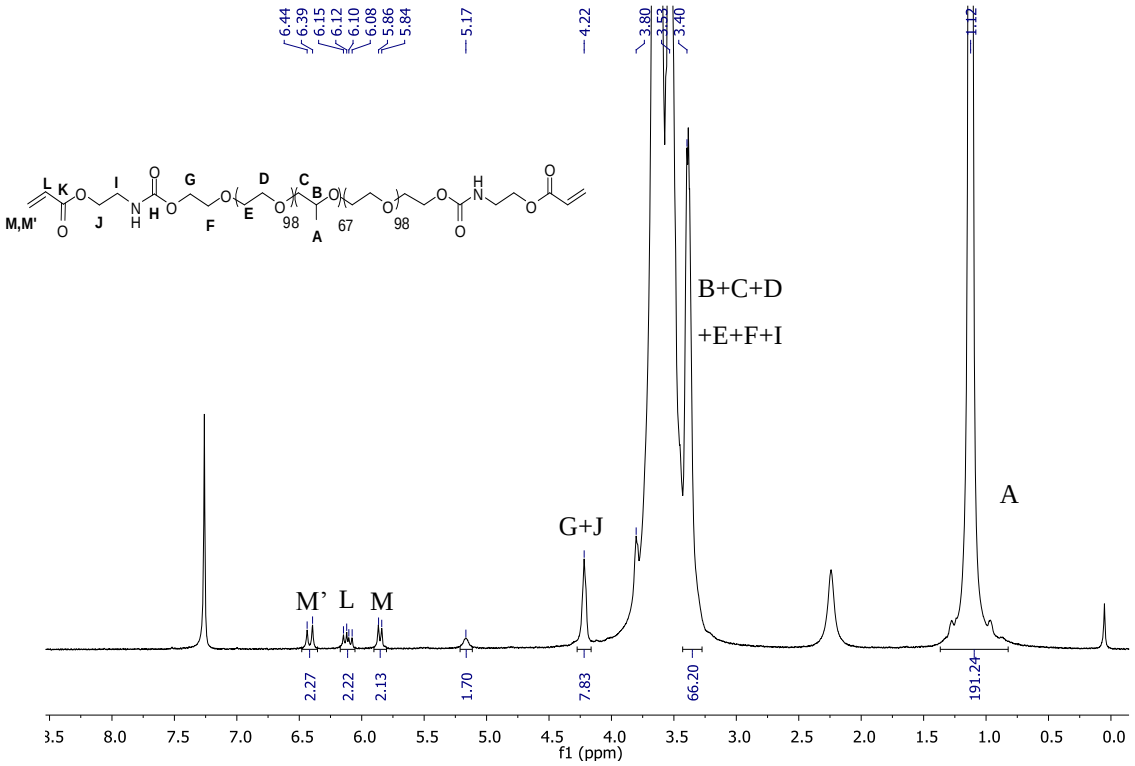

**$^{13}$C-NMR**

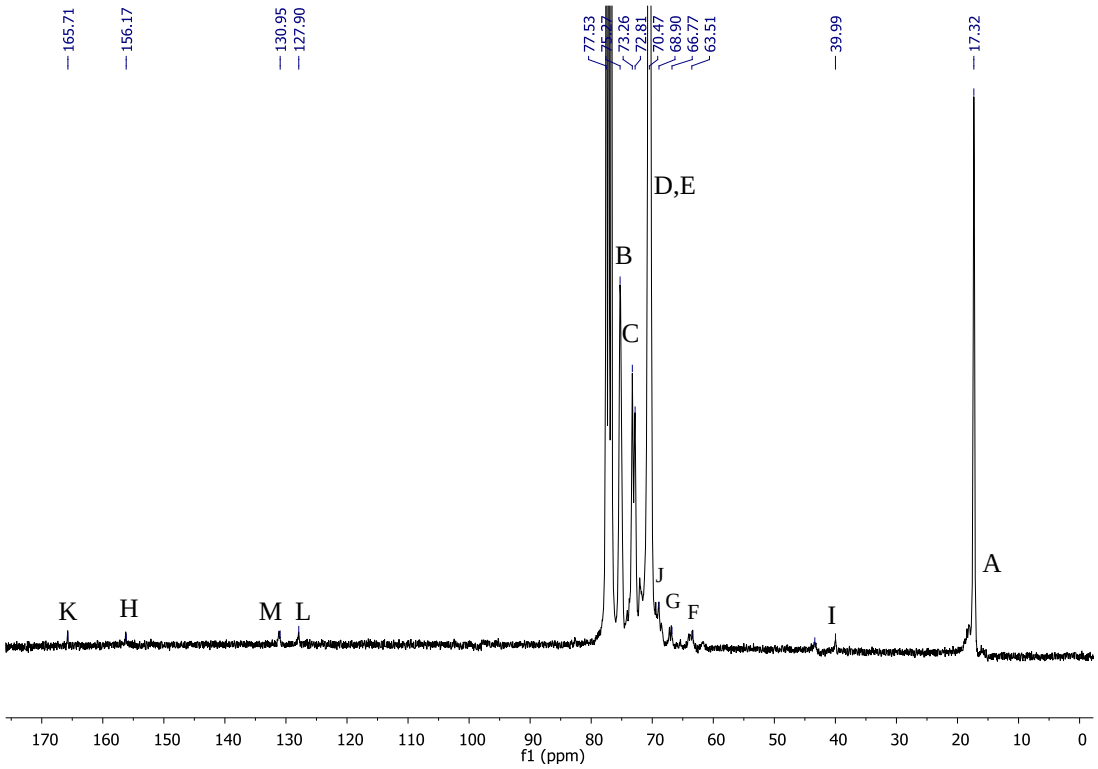
165.71
156.17
130.95
127.90
77.53
73.26
72.81
70.47
68.90
66.77
63.51
39.99
17.32
D,E
B
C
J
G
F
A
K
H
M
L
I
170
160
150
140
130
120
110
100
90
80
70
60
50
40
30
20
10
0
f1 (ppm)

**IR**

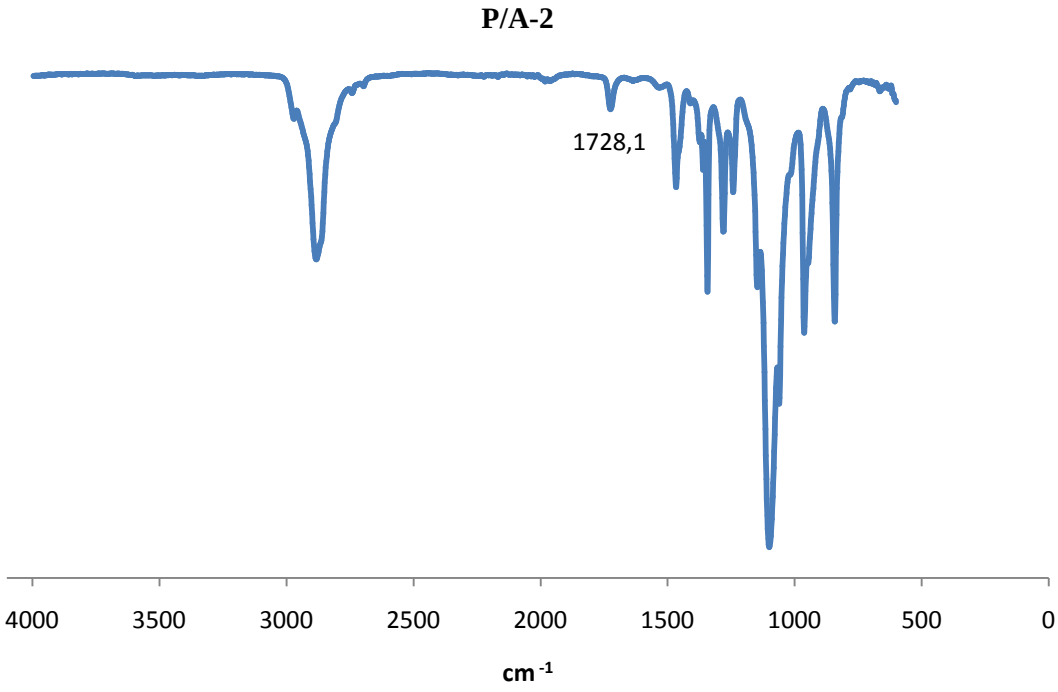
P/A-2
1728,1
4000
3500
3000
2500
2000
1500
1000
500
0
cm -1

## φ P/C-4

### $^{1}$H-NMR

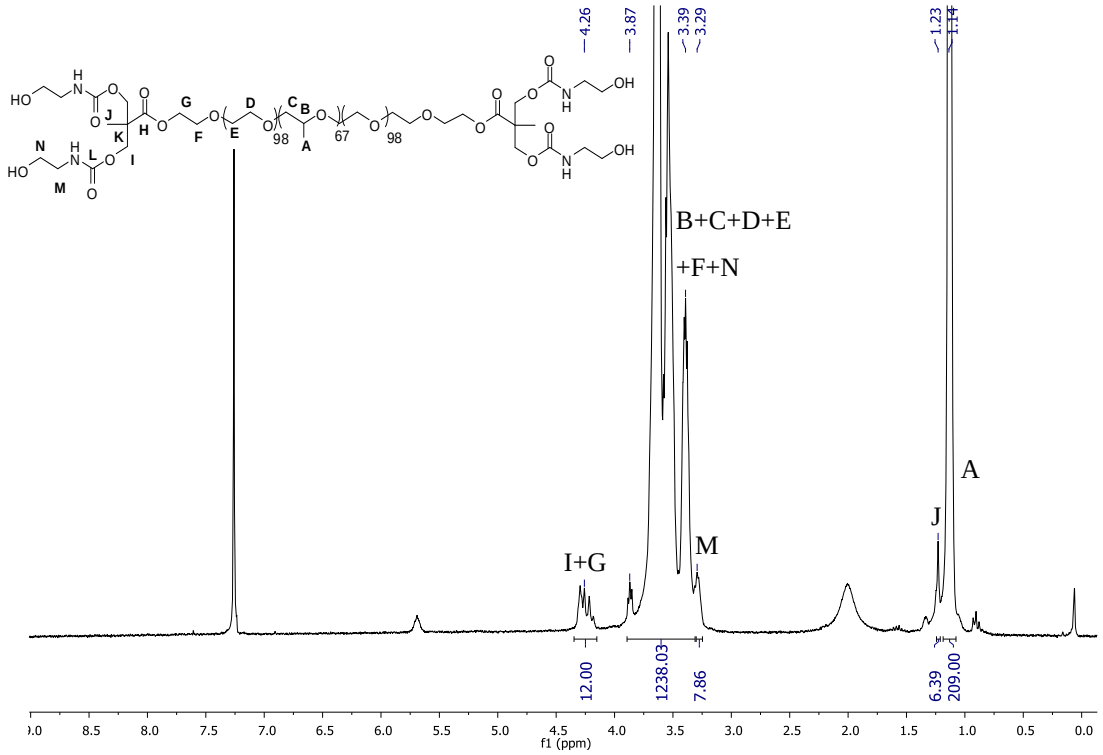


### $^{13}$C-NMR

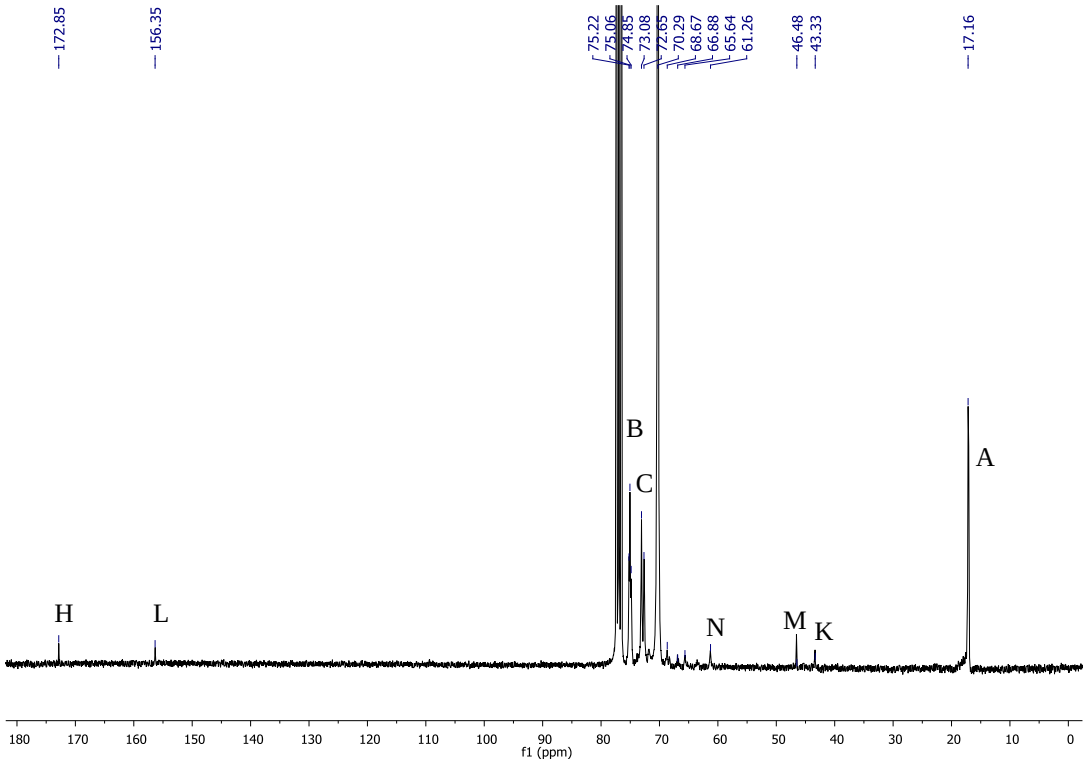

# APPENDIX 2

## ω DSC

**Pluronic F127**

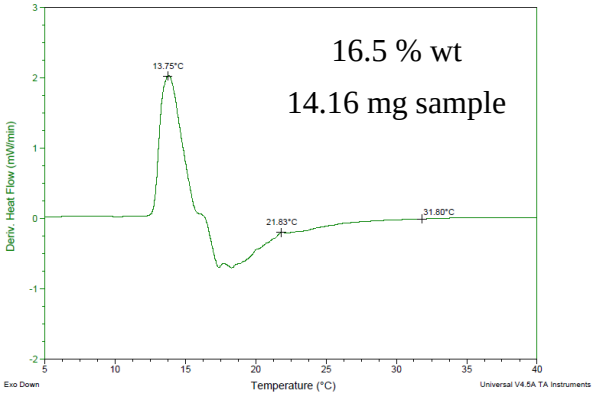


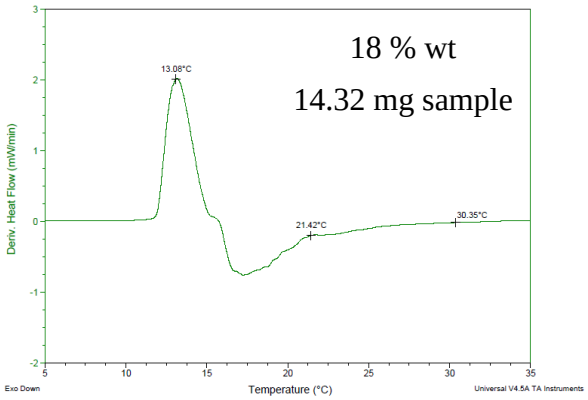


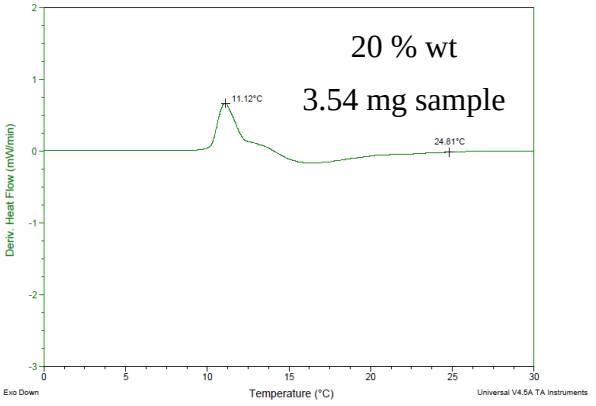


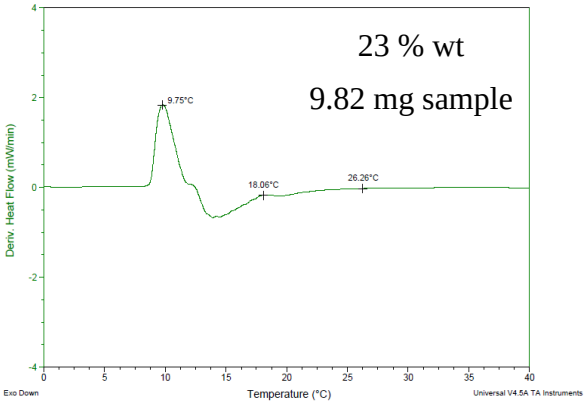


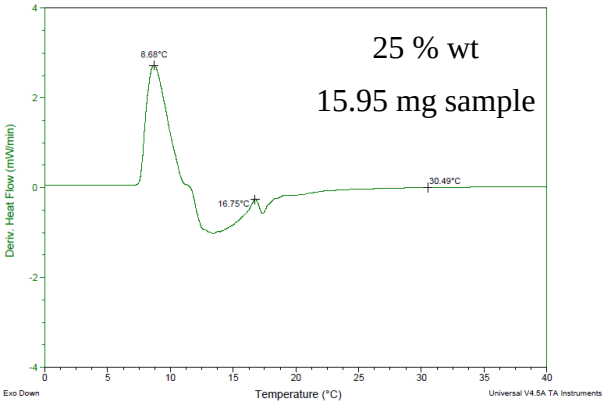

**P/C-2**

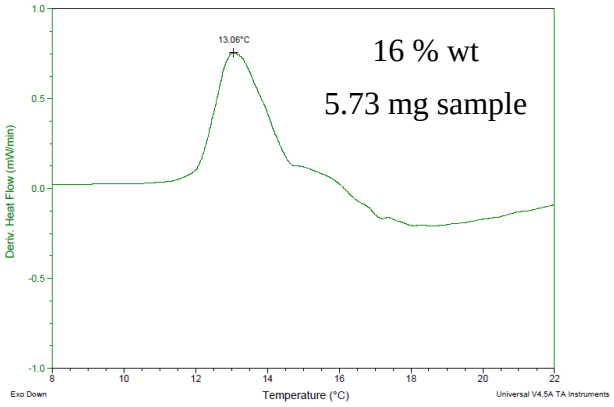
16 % wt
5.73 mg sample
13.06°C
Deriv. Heat Flow (mW/min)
Temperature (°C)
Exo Down
Universal V4.5A TA Instruments

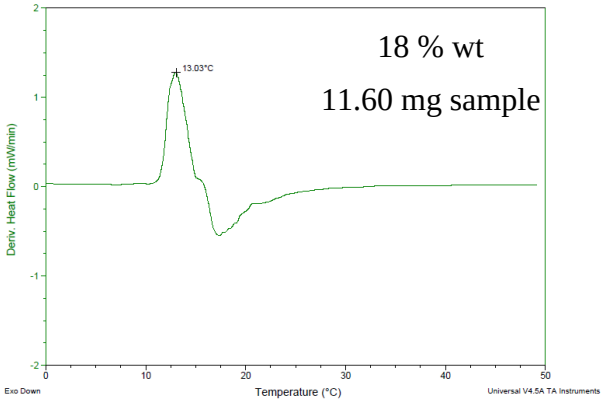
18 % wt
11.60 mg sample
13.03°C
Deriv. Heat Flow (mW/min)
Temperature (°C)
Exo Down
Universal V4.5A TA Instruments

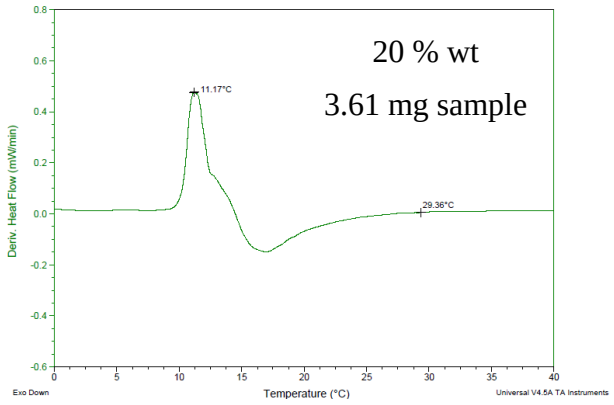
20 % wt
3.61 mg sample
11.17°C
29.36°C
Deriv. Heat Flow (mW/min)
Temperature (°C)
Exo Down
Universal V4.5A TA Instruments

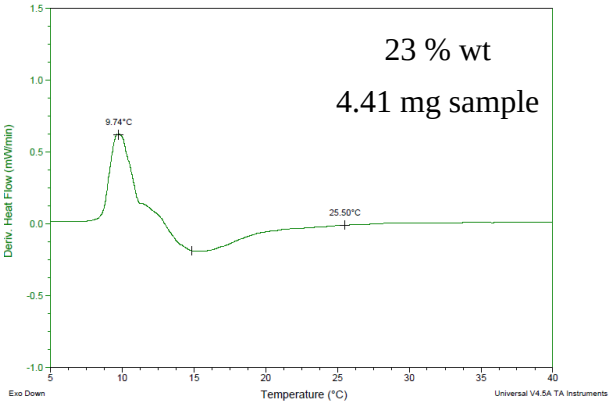
23 % wt
4.41 mg sample
9.74°C
25.50°C
Deriv. Heat Flow (mW/min)
Temperature (°C)
Exo Down
Universal V4.5A TA Instruments

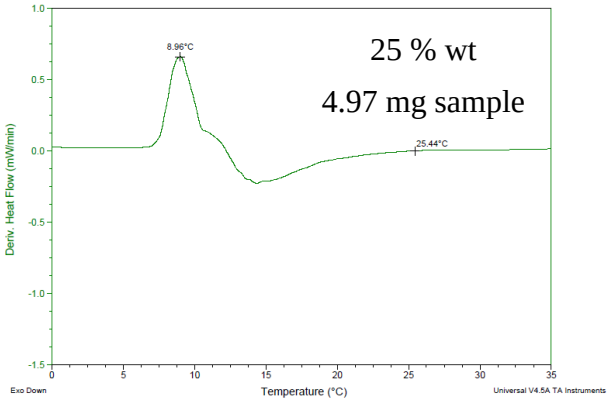
25 % wt
4.97 mg sample
8.96°C
25.44°C
Deriv. Heat Flow (mW/min)
Temperature (°C)
Exo Down
Universal V4.5A TA Instruments

**P/A-2**

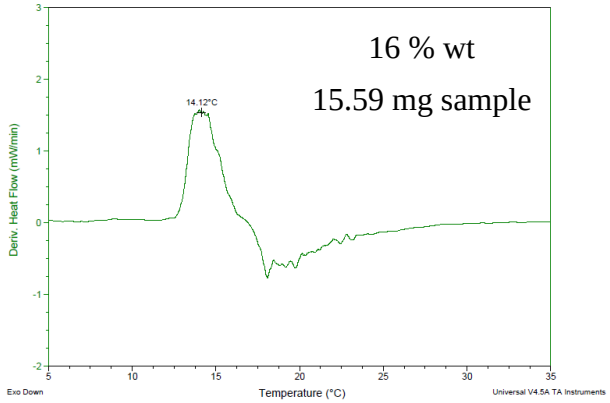
16 % wt
15.59 mg sample
14.12°C
Deriv. Heat Flow (mW/min)
Temperature (°C)
Exo Down
Universal V4.5A TA Instruments

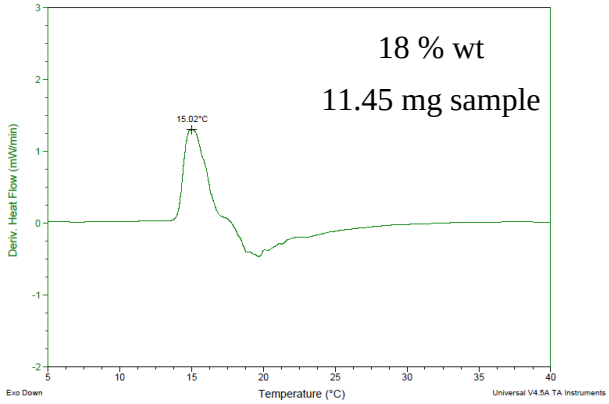
18 % wt
11.45 mg sample
15.02°C
Deriv. Heat Flow (mW/min)
Temperature (°C)
Exo Down
Universal V4.5A TA Instruments

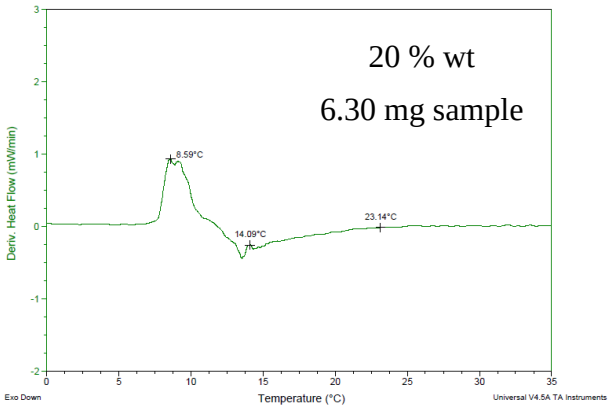
20 % wt
6.30 mg sample
8.59°C
14.09°C
23.14°C
Deriv. Heat Flow (mW/min)
Temperature (°C)
Exo Down
Universal V4.5A TA Instruments

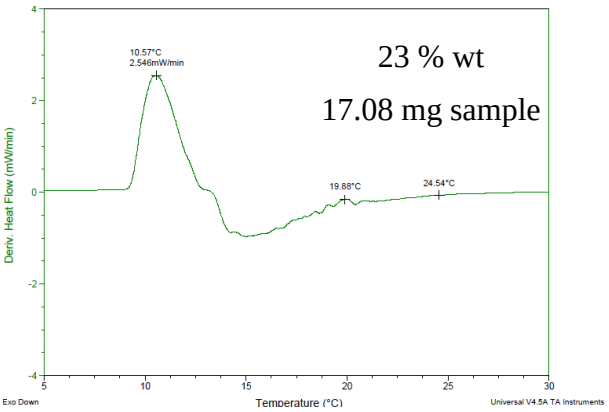
23 % wt
17.08 mg sample
10.57°C
2.546mW/min
19.88°C
24.54°C
Deriv. Heat Flow (mW/min)
Temperature (°C)
Exo Down
Universal V4.5A TA Instruments

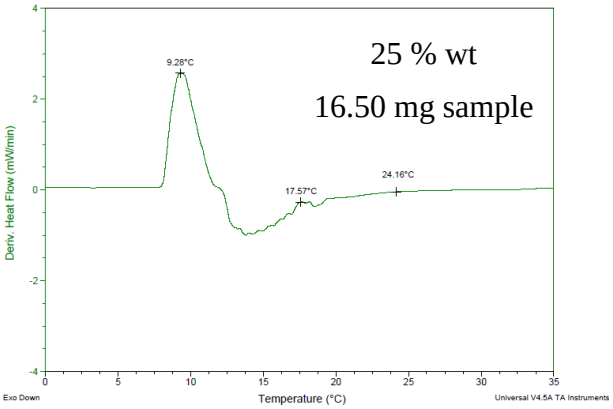
25 % wt
16.50 mg sample
9.28°C
17.57°C
24.16°C
Deriv. Heat Flow (mW/min)
Temperature (°C)
Exo Down
Universal V4.5A TA Instruments

## φ Materials and methods

*Materials:*

- All the products where purchased from Sigma-Aldrich and Acros Organics.

-The dialysis membrane was purchased from Spectrum.

*General methods*:

- $^{1}$H-NMR and $^{13}$C NMR spectra were recorded on a Bruker AV-400 (operating at 400 MHz for $^{1}$H and 100 MHz for $^{13}$C) and on a Bruker AMX300 (operating at 300 MHz for $^{1}$H and 75 MHz for $^{13}$C). $CDCl_3$ was used as solvent, chemical shifts are given ppm relative to TMS, and the solvent residual peak was used as internal standard.

- The infrared spectra of all the complexes were obtained with a Bruker Vertex 70 in ATR mode model MKII Golden Gate Single Reflection ATR System from Specac.

- Differential scanning calorimetry (DSC) was performed using a DSC Q20 V24.10 Build 122 from TA Instruments.

- Mass Spectrometry was performed using an ESI Brüker Esquire 300+, a MALDI+/TOF Brüker Microflex system.

- SEM analyses were performed with a SEM Inspect F50 with gold or platinum coated samples, at the Laboratory of Advanced Microscopy (LMA) of the INA (Nanosciences Institute of Aragon).

- TEM measurements were performed using a TECNAI G20 (FEI COMPANY), 200 kV, at the Laboratory of Advanced Microscopy (LMA) of the the INA (Nanosciences Institute of Aragon). Samples were prepared on holey carbon film 300 Mesh Cu (50) from Agar Scientific.

- DLS measurements were performed using a Brookhaven 90 Plus Particle Analyzer.

- GPC measurements were performed using a Waters e2695 Alliance liquid chromatography system equipped with a Waters 2424 evaporation light scattering detector, Styragel® columns HR1 from Waters. Measurements were performed in THF with a flow of 1mL $min^{-1}$ using polystyrene (PS) narrow molecular weight standard.

- Fluorescence measurements were performed in a Perkin Elmer LS 55 fluorescence spectrometer.

- Cells images were taken at a fluorescence inverted microscope model Olympus IX81 at CIBA (Aragon Biochemical Research Center).

### ϕ Staining for cell viability tests

- *LIVE/DEAD® Viability/Cytotoxicity Kit*

Live cells are distinguished by the presence of ubiquitous intracellular esterase activity, determined by the enzymatic conversion of the virtually nonfluorescent cell-permeant calcein AM to the intensely fluorescent calcein. The polyanionic dye calcein is well retained within live cells, producing an intense uniform green fluorescence in live cells . EthD-1 enters cells with damaged membranes and undergoes a 40-fold enhancement of fluorescence upon binding to nucleic acids, thereby producing a bright red fluorescence in dead cells. EthD-1 is excluded by the intact plasma membrane of live cells. The determination of cell viability depends on these physical and biochemical properties of cells. Cytotoxic events that do not affect these cell properties may not be accurately assessed using this method. Background fluorescence levels are inherently low with this assay technique because the dyes are virtually non-fluorescent before interacting with cells.

- *AlamarBlue®*

The assay is based on the ability of viable, metabolically active cells to reduce resazurin to resorufin and dihydro-resorufin. This conversion occurs intracellularly, where the oxidized form of the resazurin enters the cytosol and is converted to the reduced form

by mitochondrial enzyme activity by accepting electrons from NADPH, FADH, FMNH, NADH as well as from numerous cytochromes. The reduction related to growth causes the resazurin to be converted from the oxidized (or non-fluorescent) blue form to the reduced (fluorescent) red form. Since Resazurin is not-toxic to cells and is stable in culture media, continuous measurement of cell proliferation in vitro can be achieved. Toxic compounds that impair cell viability and proliferation also affect the capacity to reduce resazurin, and the rate of dye reduction is directly proportional to the number of viable cells present.